Land Surface Temperature Change in the Upper North of Bogota, Colombia from 2001 to 2020

Khodeeyoh Kasoh

A Thesis Submitted in Partial Fulfillment of the Requirements for the Degree of Master of Science in Research Methodology

Prince of Songkla University

2022

Land Surface Temperature Change in the Upper North of Bogota, Colombia from 2001 to 2020

Khodeeyoh Kasoh

A Thesis Submitted in Partial Fulfillment of the Requirements for the Degree of Master of Science in Research Methodology

Prince of Songkla University

2022

Thesis Title	Land Surface Temperature Change in the Upper North of Bogota, Colombia from 2001 to 2020
Author	Miss Khodeeyoh Kasoh
Major Program	Research Methodology

Major Advisor	**Examining Committee :**
....	....Chairperson
(Asst. Prof. Dr. Salang Musikasuwan)	(Assoc. Prof. Dr. Apiradee Saelim)
	....Committee
Co-advisor	(Asst. Prof. Dr. Salang Musikasuwan)
....	....Committee
(Asst. Prof. Dr. Rattikan Saelim)	(Asst. Prof. Dr. Rattikan Saelim)
	....Committee
	(Asst. Prof. Dr. Mayuening Eso)
	....Committee
	(Asst. Prof. Dr. Wandee Wanishsakpong)

The Graduate School, Prince of Songkla University, has approved this thesis as partial fulfillment of the requirements for the Master of Science Degree in Research Methodology.

....
(Asst. Prof. Dr. Thakerng Wongsirichot)
Acting Dean of Graduate School

This is to certify that the work here submitted is the result of the candidate's own investigations. Due acknowledgement has been made of any assistance received.

....Signature
(Asst. Prof. Dr. Salang Musikasuwan)
Major Advisor

....Signature
(Miss Khodeeyoh Kasoh)
Candidate

I hereby certify that this work has not been accepted in substance for any degree, and is not being currently submitted in candidature for any degree.

....Signature

(Miss Khodeeyoh Kasoh)

Candidate

ชื่อวิทยานิพนธ์	การเปลี่ยนแปลงอุณหภูมิพื้นผิวดินทางตอนเหนือของโบโกตา ประเทศโคลอมเบีย ตั้งแต่ปี ค.ศ. 2001-2020
ผู้เขียน	นางสาวคอดีเย๊าะ กาเสาะ
สาขาวิชา	วิธีวิทยาการวิจัย
ปีการศึกษา	2565

บทคัดย่อ

การวิจัยครั้งนี้มีวัตถุประสงค์เพื่อตรวจสอบรูปแบบและแนวโน้มตามฤดูกาลของอุณหภูมิพื้นผิวดิน (LST) และเพื่อศึกษาตัวแบบการทำนายและปัจจัยที่เกี่ยวข้องกับความแปรปรวนของอุณหภูมิพื้นผิวดินในทางตอนเหนือของโบโกตา ประเทศโคลัมเบีย ตั้งแต่ปี 2544-2563 ข้อมูลที่ใช้ในการศึกษานี้คือข้อมูล MODIS LST จากเว็บไซต์ของ NASA ซึ่งจัดเก็บเฉลี่ยทุก 8 วัน ตั้งแต่วันที่ 1 มกราคม 2544 ถึงวันที่ 27 ธันวาคม 2563 (ข้อมูลทั้งหมด 920 ค่าสังเกต) จำนวน 9 ภูมิภาค ในการศึกษานี้ใช้ฟังก์ชันเสมือนพหุนามกำลังสาม (Cubic splines functions) สำหรับการวิเคราะห์รูปแบบตามฤดูกาลและการถดถอยเชิงเส้นอย่างง่าย (SLR) เพื่อวิเคราะห์แนวโน้มการเปลี่ยนแปลงอุณหภูมิเฉลี่ยเป็นเวลา 20 ปี และพบว่าอุณหภูมิเฉลี่ยทางตอนเหนือของโบโกตาลดลงเล็กน้อยประมาณ 0.021 องศาเซลเซียสทุกปี หลังจากนั้นจะแบ่งข้อมูลออกเป็นสัดส่วน 70% : 30% สำหรับชุดข้อมูลฝึกฝนและชุดข้อมูลทดสอบตามลำดับ ในส่วนของชุดข้อมูลฝึกฝนจะนำมาใช้ในการสร้างตัวแบบการทำนายด้วยวิธีการถดถอยพหุคูณ (MLR) และการสุ่มป่าไม้ (Random Forest) และหาปัจจัยที่เกี่ยวข้องกับความแปรปรวนของอุณหภูมิพื้นผิวดิน และเปรียบเทียบประสิทธิภาพของตัวแบบแต่ละวิธีโดยใช้ค่าเฉลี่ยของรากที่สองของกำลังสองขอความคลาดเคลื่อน (RMSE) และค่าสัมประสิทธิ์การตัดสินใจพหุคูณ (R-square) ผลการวิจัยพบว่าปัจจัยที่สำคัญที่สุดในทุกภูมิภาคที่มีผลต่ออุณหภูมิพื้นผิวดินคือ ดัชนีความต่างพืชพรรณ (NDVI) และจากการเปรียบเทียบประสิทธิภาพของตัวแบบพบว่าตัวแบบการสุ่มป่าไม้มีประสิทธิภาพมากที่สุดโดยมีค่า RMSE ต่ำที่สุด และ ค่า R-square สูงที่สุดซึ่งอยู่ระหว่าง 29.90 % ถึง 53.29 % อย่างไรก็ตามไม่สามารถประกันได้ว่าตัวแบบที่ดีที่สุดจากการศึกษาครั้งนี้จะมีประสิทธิภาพดีที่สุดสำหรับพื้นที่ศึกษาอื่น ๆ

Thesis Title	Land surface temperature change in the Upper North of Bogota, Colombia from 2001 to 2020
Author	Miss Khodeeyoh Kasoh
Major Program	Research Methodology
Academic Year	2022

ABSTRACT

This purpose of this research was to examine the seasonal patterns and trends of Land Surface Temperature (LST) and to investigate the predictive models and (term lag and Normalized Difference Vegetation Index (NDVI) that related to LST variability in the upper north of Bogota, Columbia from 2001-2020. The observation data used in this study were obtained from the National Aeronautics and Space Administration (NASA) website as Moderate Resolution Imaging Spectroradiometer (MODIS) LST Data, which was collected every 8 days from January 1, 2001 to December 27, 2020 (a total of 920 data observations) from 9 regions. In this study, cubic spline was used for seasonal patterns analysis and simple linear regression was used for analyzing the trend of the average temperature change for 20 years. The results showed that the average temperature in the upper north of Bogota has been slightly decreasing, at around 0.021 degrees Celsius every year. The data has been divided into 70%-30% proportions for training and testing data sets, respectively. Multiple Linear Regression (MLR) methods and Random Forest (RF) were utilized as the prediction models and factors correlated to LST variability. Root mean square error (RMSE) and R-square were used to compare the predicting performance among constructed models. The results showed that the most important variable in all regions is NDVI. The RF model gained the smallest RMSE from testing both training and testing data sets. The R- square values of MLR model were between 23.68 % to 45.65 % while those of RF model were between 29.90% to 53.29%. However, it cannot be guaranteed that the same performance for each model will be the same for other study areas.

ACKNOWLEDGEMENT

First and foremost, I would like to thank Almighty ALLAH because this thesis work would not have been completed successfully without his blessings and guidance. I sincerely appreciate my major advisor, Asst. Prof. Dr. Salang Musikasuwan, for his inspiring guidance and kind gestures in every single way, and my co-advisors Asst. Prof. Dr. Rattikan Saelim chose for their valuable suggestions and constant encouragement throughout this research work. I also express my gratitude to Emeritus professor Don McNeil for assisting with data management and statistical analysis. Furthermore, I would like to say thank you to Assoc. Prof. Dr. Apiradee Lim, Asst. Prof. Dr. Phattrawan Tongkumchum and Asst. Prof. Dr.Rhysa McNeil for their help and for providing all the necessary support for all the students.

I would like to thank the Graduate school, Prince of Songkla University for thesis research funding. Also, I thank my friend in Department of mathematics and computer science for the assistance and stimulating discussion.

I want to express my insightful gratitude to all my friends especially, Benjamin Atta Owusu, Rusnat Nuipom, Rodiyah Sama, Nureesawati Samoh, Sufian Chema and my classmates for their immense support, and kindness in helping me to overcome any problems I have faced, and for being there for me under difficult circumstances. Many others have helped me directly and indirectly to complete this research. I thank them wholeheartedly. This acknowledgment will not be complete without expressing my deepest gratitude to my dear parents, Mr. Yeh Kasoh and Mrs. Pateemoh Kasoh, Miss. Aisyoh Kasoh, and my other family member. Thank you all.

Khodeeyoh Kasoh

CONTENTS

LIST OF TABLES

LIST OF FIGURES

Chapter 1

Introduction

1.1 Background and rationale

Land surface temperature (LST) is regarded as a significant measure of material exchange, energy balance, and biophysical and chemical processes on the land surface (Guha and Govil, 2021; Hao et al., 2016). Different Land Use/Land Cover types have different surface reflectance and roughness, which affects the LST of different surface areas (Hou et al., 2010). Recent changes in the characteristics of land surface types are the results of growing urbanization (Li et al., 2017). There has also been a significant influence of natural vegetation on the distribution of LST (Yuan et al., 2017). The Normalized Difference Vegetation Index (NDVI) has commonly been employed in LST-related research (Guha et al., 2020; Madanian et al., 2018). The LST-NDVI relationship is controlled by several variables, including thick vegetation, sand dunes, water bodies, dry soil, exposed rock surface, wetland, construction materials, etc., making it excessively complicated in nature (Qu et al., 2014; Zhou et al., 2011).

Currently, thermal infrared remote sensing has been used to determine the relationship between LST and NDVI in many studies (Deng et al., 2018; Ghobadi et al., 2015). Also, most studies have focused on major cities such as Sao Paulo in Brazil (Ogashawara et al., 2019), Bagerhat in Bangladesh (Rahman et al., 2022), Cali in Colombia (Musse et al., 2018), California (Shivers et al., 2019), and Florence and Naples in Italy (Guha et al., 2018). Within Colombia, Only only a few studies have been conducted about the seasonal relationship between LST and NDVI.

Generally, spatial and temporal sensor resolution should follow surface configurations. In any urban area, LST is highest in areas with the least number of plants (Raynolds et al., 2008). Therefore, most thermal remote sensing methods use the NDVI as the most important indicator of LST (Yuan et al., 2007), and it has been used in many studies to determine the relationship between estimated LST and NDVI

(Siddique et al., 2019; Guha et al., 2018; Son et al., 2012; Sun et al., 2007). Such as Gabriel (Parra-Henao et al., 2016), Yongming (Xu et al., 2014), and Daniel (Martnez-Bello et al., 2018), have all completed successful research projects based on the spatial-temporal relationship of LST-NDVI in Columbia. Several researchers have attempted to establish the LST-NDVI correlation (Ghobadi et al., 2015). Generally, LST has an inverse association with vegetation (Voogt and Oke., 2003). NDVI serves as a factor of LST (Goward et al., 2002). Furthermore, the LST-NDVI correlation was employed to examine the LST distribution pattern (Govil et al., 2019). A lot of recent studies look at the relationship between LST and NDVI in more than one way (Hao et al., 2019; Zhang et al., 2008).

Colombia is located in South America and is characterized as being tropical and isothermal because it's nears the equator (Romero et al., 2020). It has variations in all five regions depending on the altitude, temperature, humidity, winds and rainfall (Espinoza Villar et al., 2009). Climate change could be a problem because there isn't enough water and the land is getting worse in the high Andes mountains on the coast (Beniston et al., 2003). Rising sea levels and floods can impact communities and the economy. If climate change keeps going on, it's likely that the way it rains in Colombia will change, which will cause water shortages all over the country (Leroy, 2019). Currently, climate change is wreaking havoc in certain parts of Colombia. There have been big floods, landslides, changes in the water supply, effects on people's health, and even more big changes (Jansky et al., 2002). The Colombian government has been an ally in the country's adaptation to the effects of climate change. They are currently expanding their impact to mountainous regions in Colombia with similar social and ecological conditions to those in the capital (McGranahan et al., 2007). From the above research studies, LST and NDVI are important for Colombia. Climate development and is useful to those involved in environmental development. The main aims of the study were (1) to examine the seasonal patterns and trends of LST; and (2) to investigate the predictive models and factors (term lag and NDVI) that are related to LST variability in the upper north of Bogota, Columbia.

1.2 Objectives of Research

1. To examine the seasonal patterns and trends of LST between 2001 and 2020 in the upper north of Bogota, Colombia

2. To investigate the predictive models and factors (term lag and NDVI) that related to LST variability in the upper north of Bogota, Columbia from 2001-2020

1.3 Expected Advantages

1. Knowledge of LST's seasonal patterns and trends will be useful information for community awareness of climate changes.

2. Information related to the factors affecting LST changes may provide important information to environmental policy makers for promoting relevant projects.

1.4 Scope of the study

This study focused on LST change in the upper north of Bogota, Colombia, from 2001 to 2020. The data was retrieved from the Moderate Resolution Imaging Spectroradiometer (MODIS) terra satellite. The cubic spline function and linear regression are methods for smoothing the spline curve and extracting seasonal patterns and trends. Furthermore, a Multiple Linear Regression (MLR) model was used to determine factors related to LST. Lastly, the predictive models for LST have been developed by using MLR and Random Forest (RF) models. All statistical analyses and appropriate plots were implemented using the R program (R Core Team, 2020).

1.5 Literature review

1.5.1 MODIS satellite data

Using satellites is a sophisticated method of monitoring the Earth's climate. Since the 1950s, National Aeronautics and Space Administration (NASA) satellites have studied the Earth's atmosphere, seas, land, and snow from above the Earth's surface. Satellite-based data, such as LST and NDVI, have been widely used in various sectors, and several studies have been conducted to examine and describe their applicability (Liang et al., 2019; Seto et al., 2004; Zwally et al., 2002). Data from the MODIS Terra and Aqua sensors are often used to study climate and environmental science because they are good at picking up environmental changes caused by fire, plants, temperature, earthquakes, droughts, and floods on Earth. MODIS sensors are the most comprehensive in recording Earth's vital signals. The sensors track things like the daily percentage of Earth's surface that is cloudy, the surface temperature once every 8 days (Wang et al., 2016) and the vegetation cover once every 16 days (Testa et al., 2014). Therefore, this more accurate and less erroneous data used to determine the climatic factor shift in a bigger or smaller area.

1.5.2 Land surface temperature and Normalized Difference Vegetation Index

The NDVI remains one of the first vegetation indices established for satellite data analysis and is frequently used since it corresponds well with photosynthesis and primary vegetation production. NDVI has been observed to correlate with the canopy cover of riparian vegetation in the dry southwestern United States. Furthermore, surface and groundwater availability changes can significantly impact NDVI (Wilson et al., 2018). The NDVI is an indicator of vegetation often used to study how LST affects vegetation (Julien et al., 2006). Due to the complexity of the LST-NDVI relationship, consistent examination of such relationship is required (Deng et al., 2018).

The combined study of NDVI and LST proved to be quite valuable in identifying changes in land occupation and surface conditions by distinguishing seasonal variations from changes in land occupation (Julien et al., 2006). Land surface temperature and NDVI behaviors have also been shown to correlate (Kaufmann et al., 2003). LST is an excellent indication of the energy balance at the Earth's surface, which can offer crucial information about the surface's physical attributes and climate (Sruthi et al., 2015). Wan et al. (2004) observed changes in cover and soil moisture at many scales, indicating that the surface temperature can rise fast with water deficiency. As a result, the ratio of LST/NDVI increases during droughts. Urban planning in Monte Hermoso, Argentina involved a spatial and temporal analysis of the relationship between LST and NDVI (Ferrelli et al., 2018).

1.5.3 Statistical Methods

LST can be calculated using statistical tools and models, such as cubic spline, to investigate LST changes. Annual LST seasonal patterns can be extracted using a semi-parametric method that combines the cubic spline function with the yearly periodic boundary condition and weighted least square regression (Wongsai et al., 2017). Sharma (2018) applied linear regression model to examine the seasonal trends and patterns of LST and found inter-annual temporal trends and intra-annual seasonal patterns in LST over Kathmandu Valley, Nepal. Results from Kavitha et al. (2016) indicate that linear regression models perform better at modelling LST than time series models because the former accounts for various dependent variables.

Random forest (RF) is a popular method for machine learning that can be used to create prediction models. Random forests were first introduced by Breiman in 2001 (Breiman, 2001). RF consists of classification and regression trees (Speiser et al., 2019). The formal structure of the Random Forest Regression is shown in Figure 1.1. RF models can identify complex associations between input parameters and massive numbers of observations (Karimi et al., 2021). The heating values of solid waste in an incinerator were predicted using four machine learning algorithms are artificial neural network, Adaptive neuro fuzzy inference system, Support vector machine, and RF. You et al. (2017) compared these techniques, and the RF model was found to be the most balanced model in terms of prediction accuracy and training time.

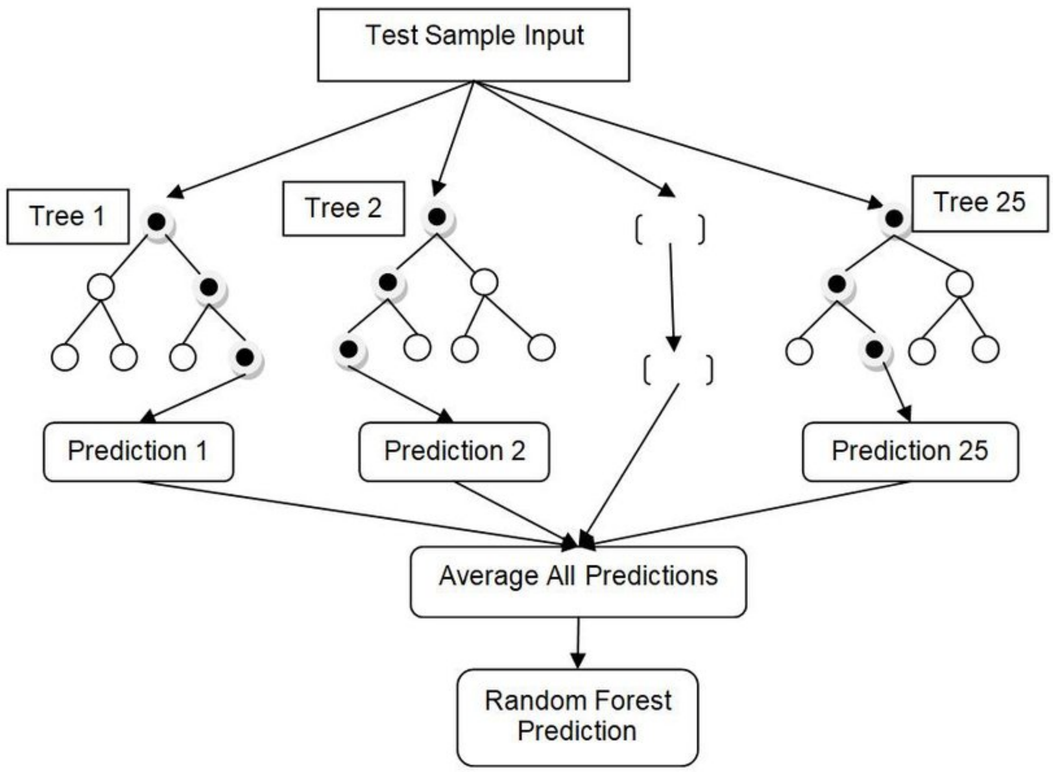

Figure 1.1 The formal structure of the Random Forest Regression

1.6 Conceptual framework

The study's conceptual framework is shown in Figure 1.2 below to illustrate the methodological processes of the investigation.

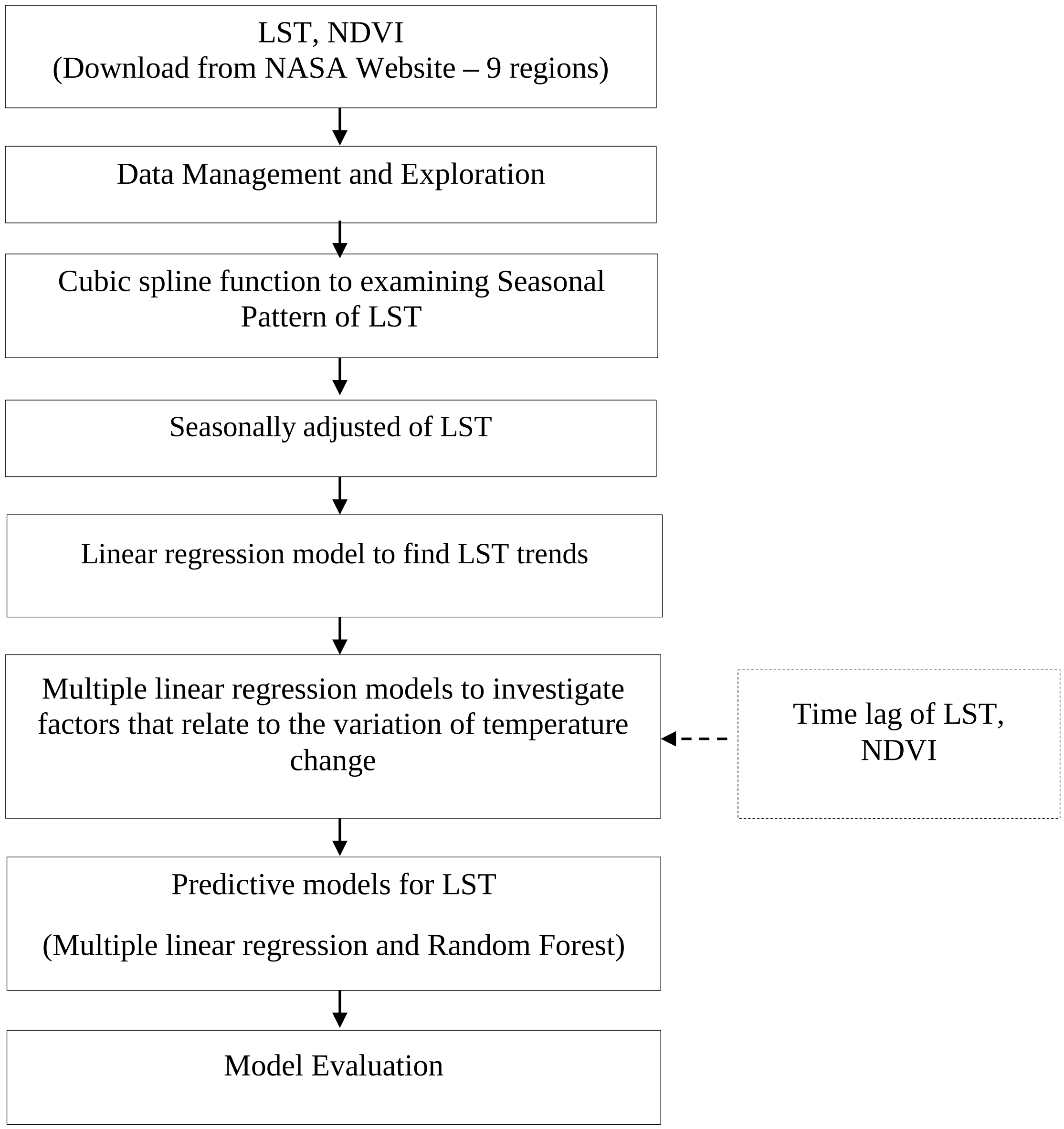

Figure 1.2 Data analysis diagram

1.7 Organization of the thesis

This thesis comprises four chapters, and their details are described below: Background and rationale, research objectives, expected advantages, literature review, the scope of the study, conceptual framework, and organization of the thesis are in chapter 1. In Chapter 2, the method is explained. These methods include the area of study, the data used, and the analytical techniques. Chapter 3 is about the results of modeling seasonal patterns and trends with cubic spline, linear regression, factors related to LST, LST predictive models, and a comparison of how well the models work. Chapter 4 presents the discussion and conclusion of the research findings, the limits of the research, and future studies for technique improvement.

Chapter 2

Methodology

This chapter details about research methodologies used to complete this study. It describes the study area, data sources, management, and statistical methods.

2.1 Study area

The study area is the city in the upper north of Bogota, Colombia (Figure 2.1), situated in the savannah biome inside the eastern mountain range of the Andes Mountains. Most of the city's territory is flat, bounded on the east by hills and mountains and on the west by the Bogota River and its wetlands. The entire urban population is around 7.9 million people (Ramirez-Aguilar et al., 2019), and the local climate is determined by two primary factors: latitude and elevation. The elevation of Bogota is 2,600 meters above sea level. Bogota's average annual temperature is just 14.2 degrees Celsius (°C), with a mean low of 8.4 °C and a mean high of 19.7 °C. The climate in the area is subtropical highland, which is oceanic rather than tropical (Natarajan et al., 2015).

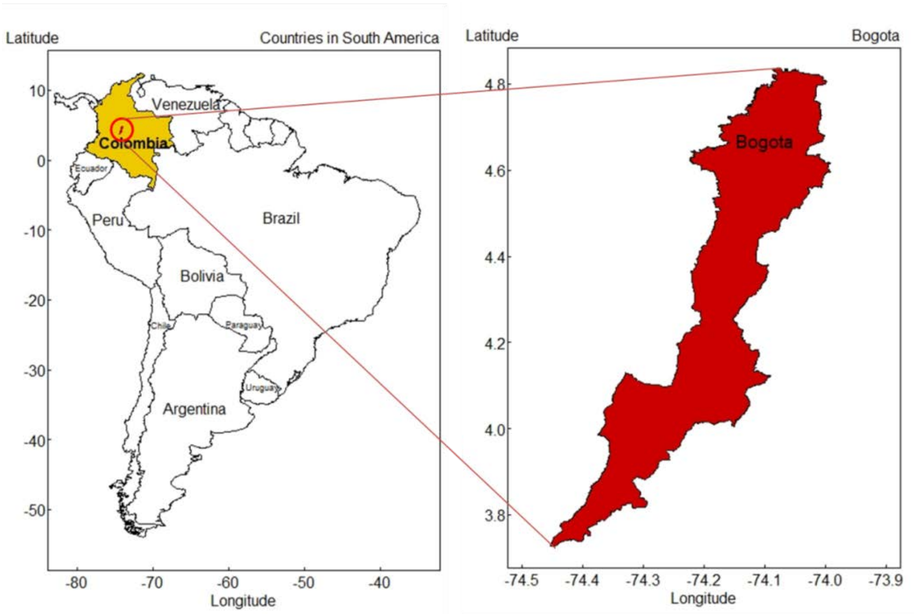

Figure 2.1 Locations of the study area

2.2 Data source

The NASA satellites is built with a Terra sensor. MODIS LST and NDVI products with codes MOD11A2 and MOD13Q1, respectively, are the land product subsets of the terra platform. These were temperature and vegetation products on its website and with its documentation.

2.2.1 Land Surface Temperature (LST) data

Two decades of LST data observations were obtained from 2001 to 2020. Daytime data with a spatial resolution of 1 km2 are included in MOD11A2 LST products (Wang et al., 2020; Gidey et al., 2018; Zhang et al., 2014). The data values are measured on the Kelvin scale. As LST data are 8-day average temperature observations, thus, there are 46 observations each year and 920 observations over 20 years. For each region, the data consisted of 7×7 = 49 km^2 and 49 pixels, each pixel of 1×1 km^2 (Figure 2.2). As a data frame, each region is represented by a matrix of 49 pixels × 920 observations. The first six columns (Table 2.1) describe the data attributes (V1 to V6), whereas the remaining columns are the LST values (t1 to t49).

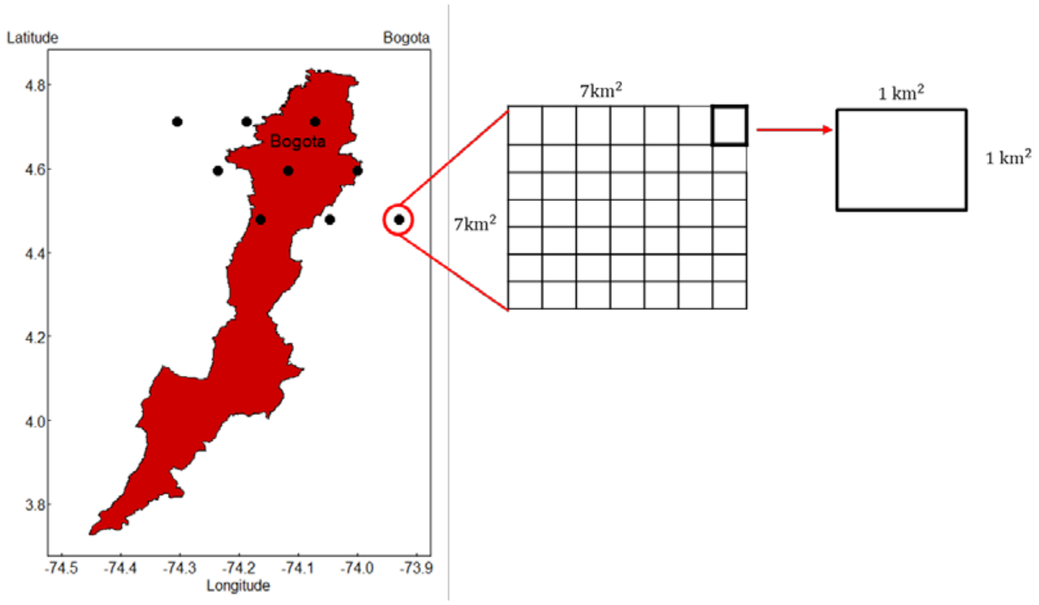

Figure 2.2 The upper north of Bogota each region

Table 2.1 Structure of LST data for a subregion from MODIS

Observations	variable					
	V1	**V2**	**V3**		**t48**	**t49**
1	MOD11A2…	MOD11A2	A2000049	. . .	F	F
2	MOD11A2…	MOD11A2	A2000057	. . .	F	299.02
3	MOD11A2…	MOD11A2	A2000065	. . .	298.08	299.34
.	.	.	.			
.	.	.	.			
.	.	.	.			
919	MOD11A2…	MOD11A2	A2020353	. . .	295.18	296.12
920	MOD11A2…	MOD11A2	A2020361	. . .	297.96	298.54

2.2.2. Normalized Difference Vegetation Index) (NDVI)

The MOD13Q1 product provides the NDVI data. The data were recorded at 16-day intervals from 2001 to 2020 over 9 regions, measuring with a spatial resolution of 250 m^2 (Ruan et al., 2020; Testa et al., 2014; Jin et al., 2014). There are 23 observations per year and 460 observations in 20 years. The data for NDVI and LST covered different areas. Each region was 33 ×33, denoted by 1,089 pixels. As a data frame for each region had a matrix of 1,089 picels×460 observation. And first 6 columns (A1 to A7) describe the data characteristics, while the remaining columns (V1 to V1089) were the NDVI values (Table 2.2).

Table 2.2 Structure of NDVI data for a subregion from MODIS website

Observations	Variables					
	A1		V1	…	V1088	V1088
1	MOD13Q1.A2000049…	…	0.14	…	0.17	0.27
2	MOD13Q1.A2000065…	…	0.68	…	0.2335	0.24
3	MOD13Q1.A2000081…	…	0.08	…	0.3275	0.30
.						
.						
.						
459	MOD13Q1.A2020337…	…	0.63		0.26	0.31
460	MOD13Q1.A2020353…	…	0.48		0.28	0.28

2.3 Data management

Table 2.3 shows the LST data structure of a region after the first six columns had been removed and 49 pixels averaged into one value per day. The data values were converted from Kelvin to Celsius scale by subtracting 273.5

Table 2.3 The average of LST for each region

Observation	Year	Day	Reg.1	Reg.2		Reg.8	Reg.9
1	2001	1	27.34	27.79	...	21.06	26.79
2	2001	9	27.10	27.33	...	23.02	28.47
3	2001	17	30.63	27.07		18.78	27.21
⋮	⋮	⋮	⋮	⋮		⋮	⋮
919	2020	353	22.88	25.80	...	15.09	24.55
920	2020	361	25.80	25.12	...	12.67	20.34

The data for NDVI was in the upper north of Bogota. The data period is the same as LST (beginning on January 1, 2001 and ending on December 19, 2020). In managing NDVI data to match with the LST pixel, we found the right key pixel, which ranged from 1 to 16. In our area, pixel number 6 was identified as an acceptable key pixel for NDVI and LST data merging (Figures 2.3), which is the NDVI pixel, one of 16 that correspond to a LST pixel. Therefore, NDVI pixels outside LST sub-regions are trimmed. To begin, 28×28= 784 pixels were systematically selected from each region for analysis.

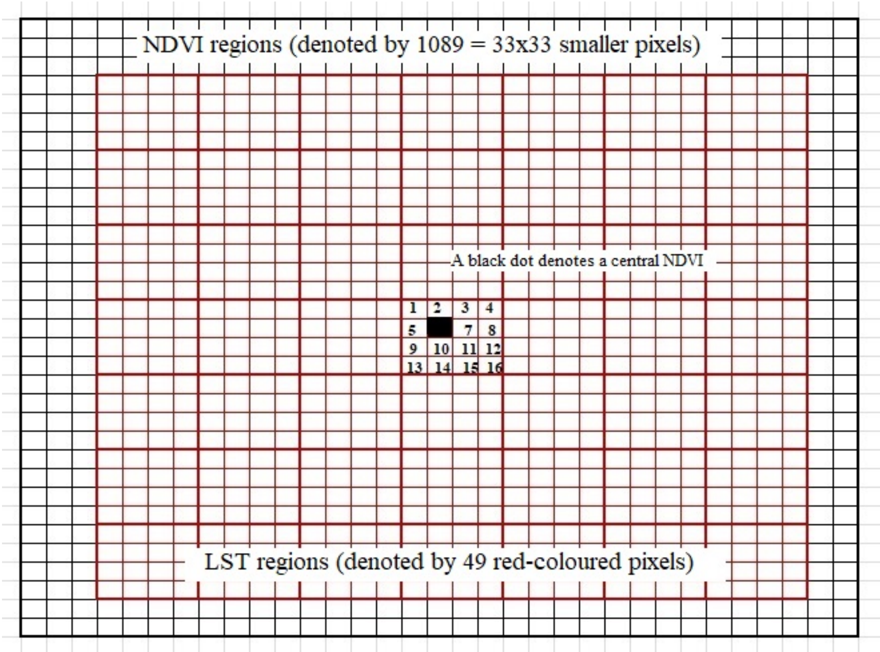

Figure 2.3 LST and NDVI pixel numbers and sizes (example of central pixel)

Table 2.2 shows the NDVI data structure of a region after eliminating the first seven columns and selecting 784 pixels as data variables for each region. After that, we manage data by 784 pixels and choose the median value of 784 pixels as data. Every 16 days, we only get one NDVI, so each region has 460 observations.

Table 2.3 The average of NDVI for each region

Observation	**Year**	**Day**	**Reg.1**	**Reg.2**		**Reg.8**	**Reg.9**
1	2001	1	0.70	0.71	...	0.59	0.69
2	2001	17	0.76	0.70	...	0.55	0.70
3	2001	33	0.69	0.66		0.50	0.69
⋮	⋮	⋮	⋮	⋮		⋮	⋮
459	2020	337	0.64	0.66	...	0.59	0.68
460	2020	353	0.62	0.65	...	0.49	0.65

2.4 Statistical methods

The natural cubic spline with a linear function was used to examine the trends and seasonal patterns of LST in each region using adequate number of knots, the time series plot was generated for LST. The knot positions were fixed to smoothen the spline curve. A cubic spline function formula is shown in the equation (2.1)

$$S_i = \alpha + bt_i + \sum_{k=1}^{p} C_k \left(t_i - t_k\right)_+^3 \qquad (2.1)$$

Where S_i is the spline function, α, b and C_k are the parameters in the model. k is knot location, t_i denotes time in average every 8 days, that is specified from 20 year, $t_1 < t_2 < \ldots < t_p$ are specified knots and $\left(t_i - t_k\right)_+$ means that $\left(t_i - t_k\right)$ is positive for $\left(t_i > t_k\right)$ and zero otherwise. After that, the LST data were seasonally adjusted by subtracting the fitted values from the observed LSTs using the formula in Equation 2.2 below:

$$Z_i = x_i - S_i + \overline{x} \qquad (2.2)$$

Where, Z_i is the seasonal adjusted LST at observation i, x_i is the LST observation, S_i is the fitted value from the spline model and $\overline{x}$ is the observed LST overall mean.

A linear regression model incorporating the filtered autocorrelation in seasonally adjusted average 8-day LST was used to examine the LST from 2001 to 2020 in 9. The simple linear regression using the formula in Equation 2.3 below:

$$\hat{y}_t = a + bt \qquad (2.3)$$

Where, $\hat{y}_t$ is the predictions value at the time t , a is the intercept, b is the regression coefficient in time (average 8 day), t is the time $\left(t = 1, 2, 3, \ldots, 920\right)$.

The prediction models and parameters that correlate to LST variability in the upper north of Bogota utilize MLR methods and RF. The MLR equation has the same shape as the simple linear regression equation but has more terms. The formula that follows:

$$\hat{y}_t = a + b_1 y_{t-1} + b_2 y_{t-2} + b_2 y_{t-3} + b_4 NDVI \tag{2.4}$$

RF predictions are produced independently for each regression tree, followed by an arithmetic average of the trees as the final forecast. The main equation providing the final RF forecast for regression results based on constructed trees is as follows:

$$F(x) = \frac{\sum_{j=1}^{N} T_j(X)}{N} \tag{2.5}$$

Where N indicates number of trees, T_j represents each tree and F is a prediction at a new point x as an averaged prediction based created trees (Hastie et al., 2009).

After obtaining the appropriate models, the predicted value is calculated from the training and testing datasets and evaluating those models using RMSE as shown in

Equation.

$$RMSE = \sqrt{\sum_{t=1}^{n} \frac{(y_t - \hat{y}_t)^2}{n}} \tag{2.6}$$

Where n is defined as the number of predicted data, t is defined time, y_t is observation at time t, and $\hat{y}_t$ is predicted value. Finally, the final models were tested using R-Squared to determine whether they fit well enough for the training dataset. All statistical analyses and graphical presentation were carried using the R statistical program (R Development Core, 2020).

Chapter 3

Results

This chapter presents the results of an eight-day average land surface temperature data analysis in Bogota. It consists of descriptive summary of the LST data, LST seasonal patterns and trend analyses, factors that are related with LST changes, as well as the LST predictive models, and their performance comparison.

3.1 Data Summary

Based on the 20-year LST data from Bogota over 9 regions, the minimum average LST (16.66 ℃) was observed in region 6, where the LST ranged from 0.41 ℃ to 28.39 ℃. The LST in region 1 ranged between 11.59 ℃ and 35.79 ℃, with an average of 23.70 ℃. The highest average LST was 38.35℃, recorded over region 5, while the minimum average LST was 0.41 ℃ in region 6. Numerical summaries of the LST in each region are shown in Table 3.1.

Table 3.1 Data summaries of average LST of each region

Region	**Latitude**	**Longitude**	**Mean (℃)**	**Min (℃)**	**Max (℃)**
1	4.712	-74.305	23.70	11.59	35.79
2	4.712	-74.188	24.48	12.16	34.05
3	4.712	-74.071	26.24	11.37	35.08
4	4.596	-74.235	24.50	9.73	33.78
5	4.596	-74.117	27.58	9.58	38.35
6	4.596	-74.000	16.66	0.41	28.39
7	4.479	-74.164	19.14	1.57	33.41
8	4.479	-74.047	17.75	4.41	28.83
9	4.479	-73.930	24.59	8.84	35.96

3.2 LST Seasonal pattern and trend analysis

The seasonal trends of LST averaged over 20 years in 9 regions are shown in Figure 3.1. The temperature in °C is shown by the Y-axis while the day of the year is represented by the X-axis. Each column of the plot represents the LST in each region. The cubic spline function was fitted to the LST seasonal patterns. The spline curve is shown in the red line. Besides, eight knots placed on days 10, 40, 80, 130, 240, 290, 330, and 360 were selected to fit to smoothen the spline curve. The positions of the knots are shown with the plus (+) symbol. The adjusted r-squared (R^2) from linear regression and eight-knot cubic spline models, which measure the goodness of seasonal components fitted to raw LST in each region, were reported. Figure 3.1 shows that seasonal patterns are consistent throughout the year, with the coldest period happening in the middle of the year and the hottest periods occurring in December and March. The lowest temperature occurs in the middle of the year.

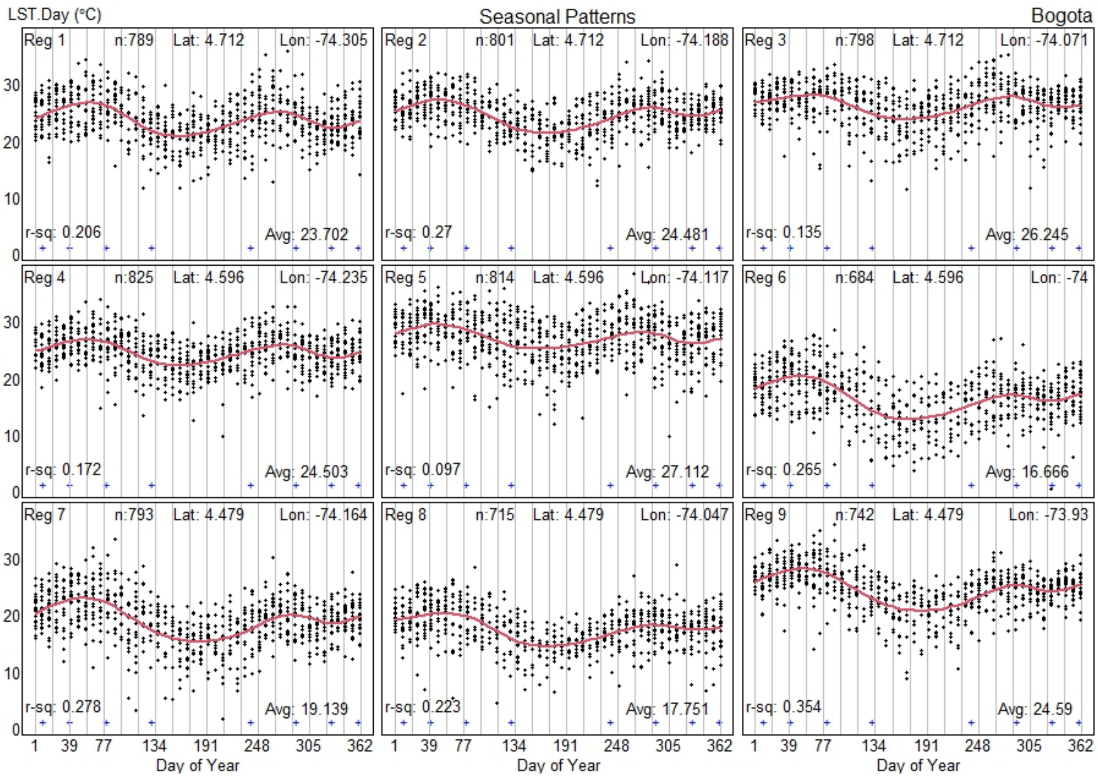

Figure 3.1 Seasonal LST pattern in Bogota for 9 regions

A simple linear regression model was used to observe the trend of LST. The data were plotted, and the annual seasonal fluctuation of LST, derived from the natural cubic spline function, was added back in and colored red to explain the LST trend over a 20-year period. In Figure 3.2, grey dots are data plotted by year. The increasing or decreasing trend (Inc/dec) per decade and respective p-values from simple linear regression show how much LST has changed from 2001 to 2020. As shown in Figure 3.2, in regions 2 and 4, the temperature increase was not statistically significant, and the temperature decline was statistically significant in the remaining regions. The equations of simple linear regression for 9 regions were given in Table 3.2.

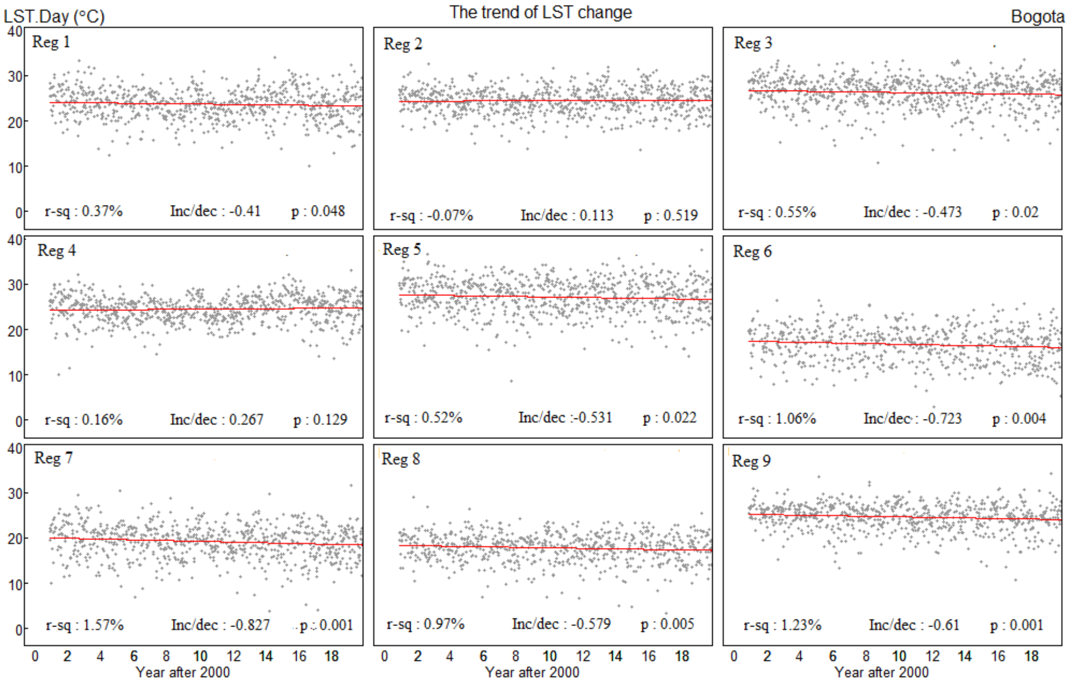

Figure 3.2 Trend patterns of 9 regions

Table 3.2 The equation of simple linear regression for 9 regions

Region	**Equation**
1	$\hat{y}_t = 24.11578 - 0.00089t$
2	$\hat{y}_t = 24.37482 + 0.00024t$
3	$\hat{y}_t = 26.72402 - 0.00102t$
4	$\hat{y}_t = 24.23180 + 0.00058t$
5	$\hat{y}_t = 27.65331 - 0.00115t$
6	$\hat{y}_t = 17.40047 - 0.00157t$
7	$\hat{y}_t = 20.00248 - 0.00180t$
8	$\hat{y}_t = 18.34220 - 0.00126t$
9	$\hat{y}_t = 25.20530 - 0.00132t$

Table 3.2 shows that the temperatures have increased in Regions 2 and 4. Simultaneously, temperatures decreased in other regions significantly.

3.3 Factors that related to LST

The historical data of both LST and NDVI were examined to determine variables associated with LST changes. The ARIMA model was used to find the appropriate historical LST data. This was determined by analyzing the Autocorrelation Function (ACF) and Partial Autocorrelation Function (PACF) graph for all regions. Figure 3.3-3.4 demonstrates that the AR(3) or lag term 3 is appropriate to be considered for factors related to LST.

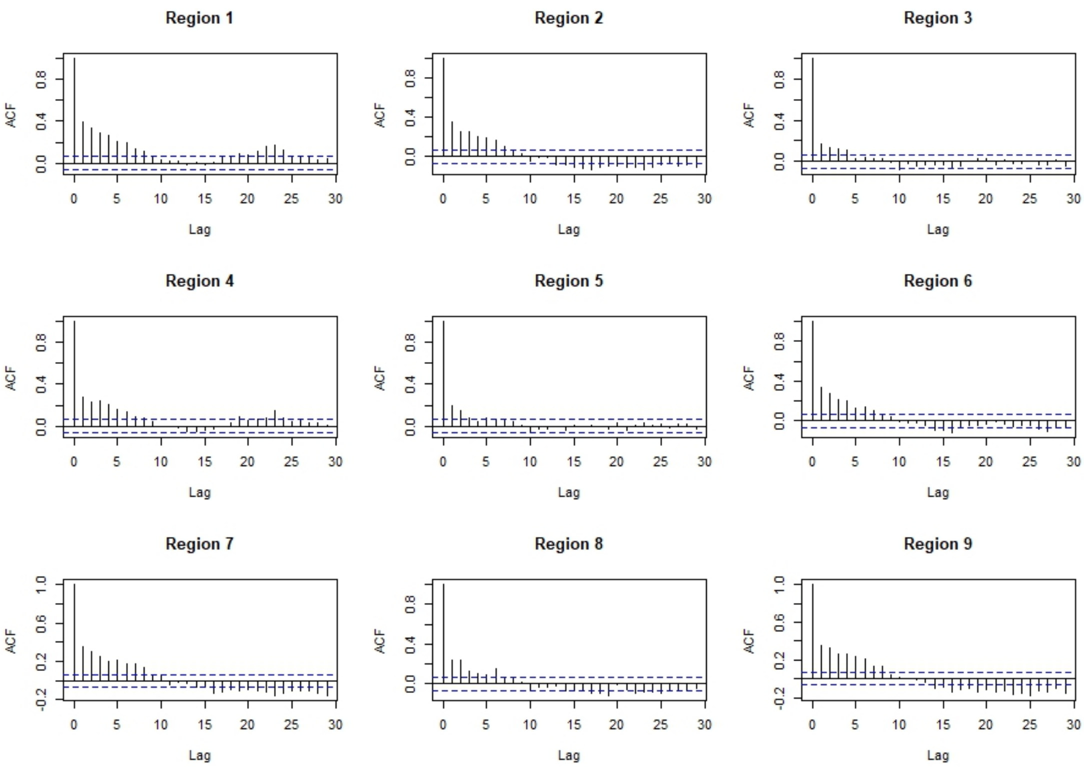

Figure 3.3 The graph of Autocorrelation Function (ACF)

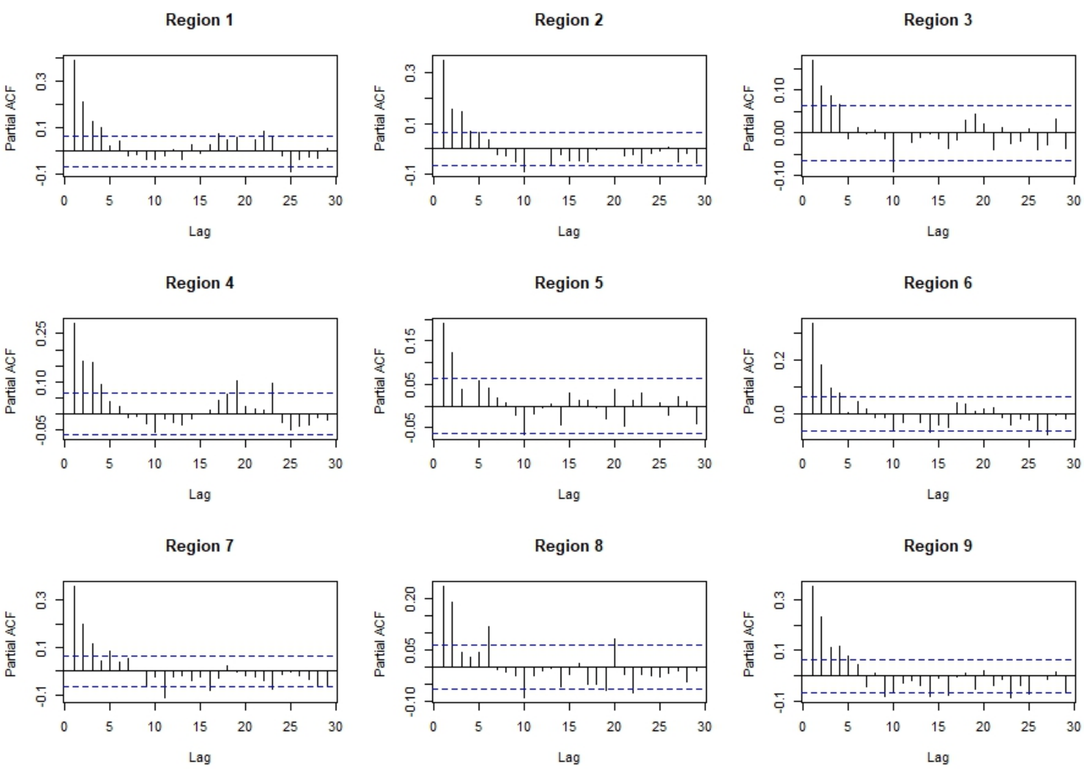

Figure 3.4 The graph of Partial Autocorrelation Function (PACF)

MLR and RF were used to find factors related to LST. The equation of MLR for 9 regions was given in Table 3.3.

Table 3.3 The equation of factors that related to LST

Region	Equation
1	$\hat{y}_t = -2.12 + 0.15y_{t-2} + 0.06y_{t-3} + 31.95ndvi_t$
2	$\hat{y}_t = -1.98 - 0.12y_{t-1} + 0.09y_{t-2} + 0.12y_{t-3} + 36.29ndvi_t$
3	$\hat{y}_t = 6.59 + 0.11y_{t-2} + 0.08y_{t-3} + 20.87ndvi_t$
4	$\hat{y}_t = 0.97 - 0.11y_{t-1} + 0.15y_{t-2} + 34.20ndvi_t$
5	$\hat{y}_t = 2.54 - 0.22y_{t-1} + 0.13y_{t-2} + 38.51ndvi_t$
6	$\hat{y}_t = -0.95 + 0.15y_{t-2} + 0.14y_{t-3} + 24.40ndvi_t$
7	$\hat{y}_t = -2.74 - 0.15y_{t-1} + 0.16y_{t-2} + 0.07y_{t-3} + 35.86ndvi_t$
8	$\hat{y}_t = 0.83 + 0.21y_{t-2} + 24.30ndvi_t$
9	$\hat{y}_t = 2.32 + 0.20y_{t-1} + 0.21y_{t-2} + 0.08y_{t-3} + 15.03ndvi_t$

For RF, the first step is to choose a subset of the data at random sampling with replacement. Determine a number of trees as can be seen in Figure 3.4, we decided to use a number of trees of 500 for this dataset. Decision tree for each data set, we will randomly select a variable by “ $\sqrt{\mathrm{V}}$ ” (V is variable), the average chosen prediction result the final decision.

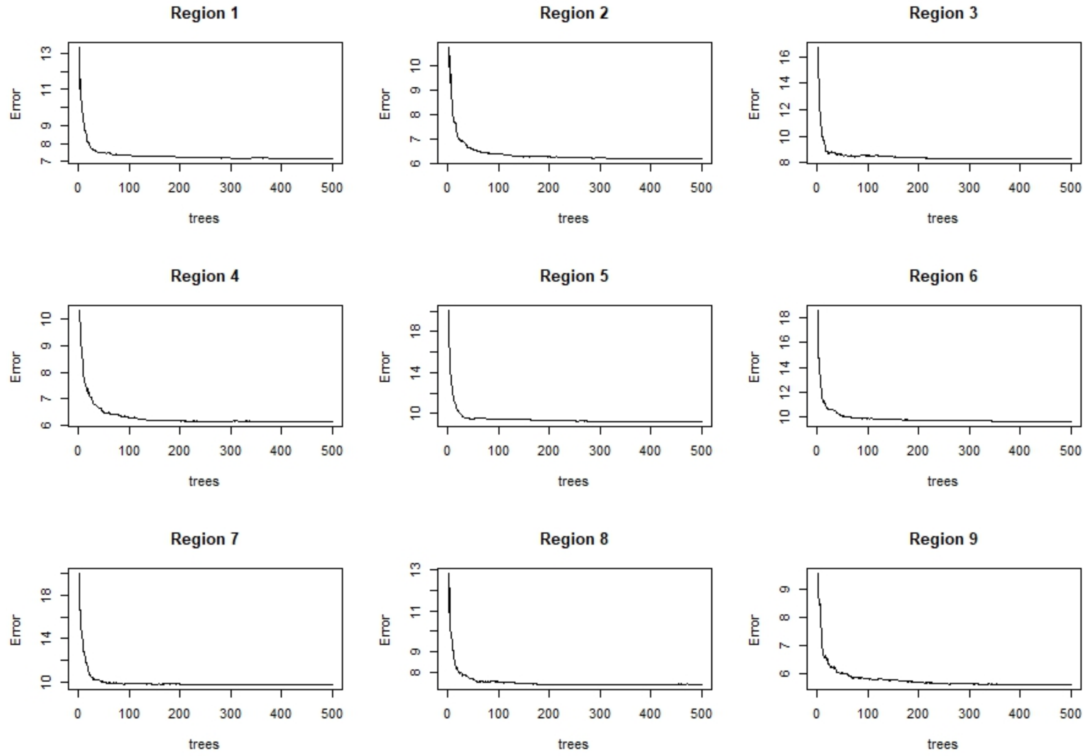

Figure 3.5 Set the number of trees for the RF.

Figure 3.6 explains the important measure for each variable of a factor related to LST according to Mean Decrease Accuracy (%IncMSE). The higher the value of the mean decrease accuracy, the greater the importance of the variable in the model. The most important variable in all regions is NDVI.

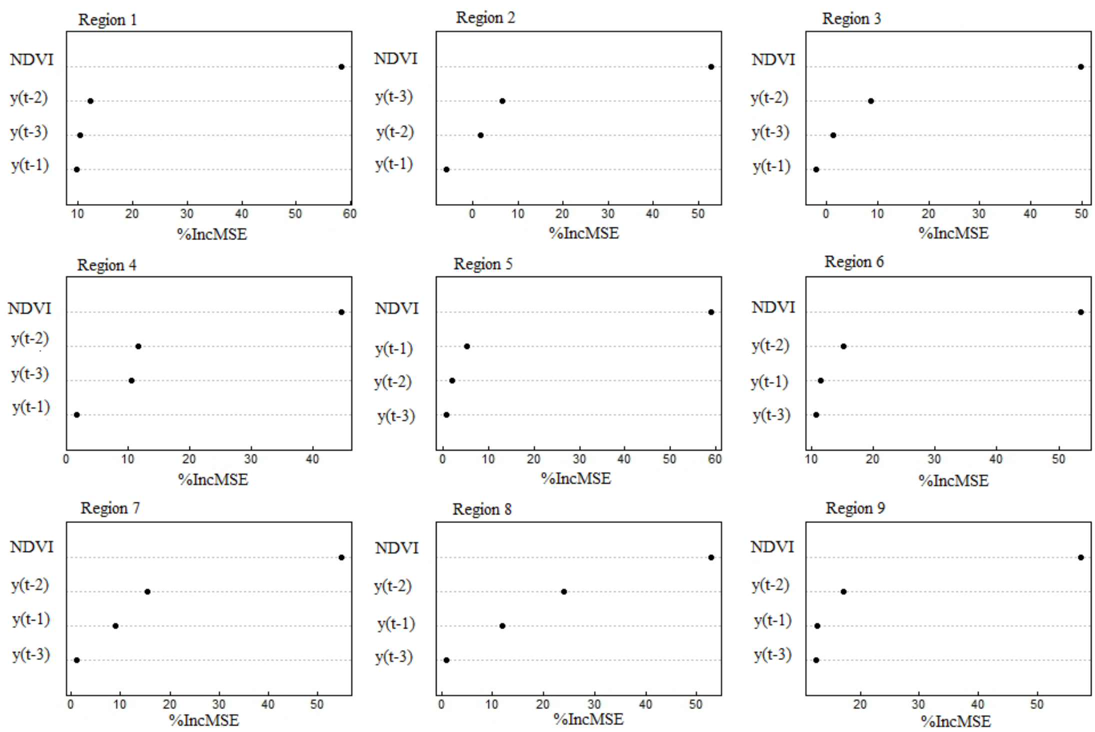

Figure 3.6 The important measure for each variable of factor related to LST according to %IncMSE for 9 regions

3.4 LST predictive models

The plots of predicted LST against original data for all regions using the Multiple Linear Regression model and Random Forest have been presented in Figure 3.7 and 3.8. Each blue line represents the original LST, the red line represents the predicted LST for the training dataset and the green line represents the predicted LST for the testing dataset.

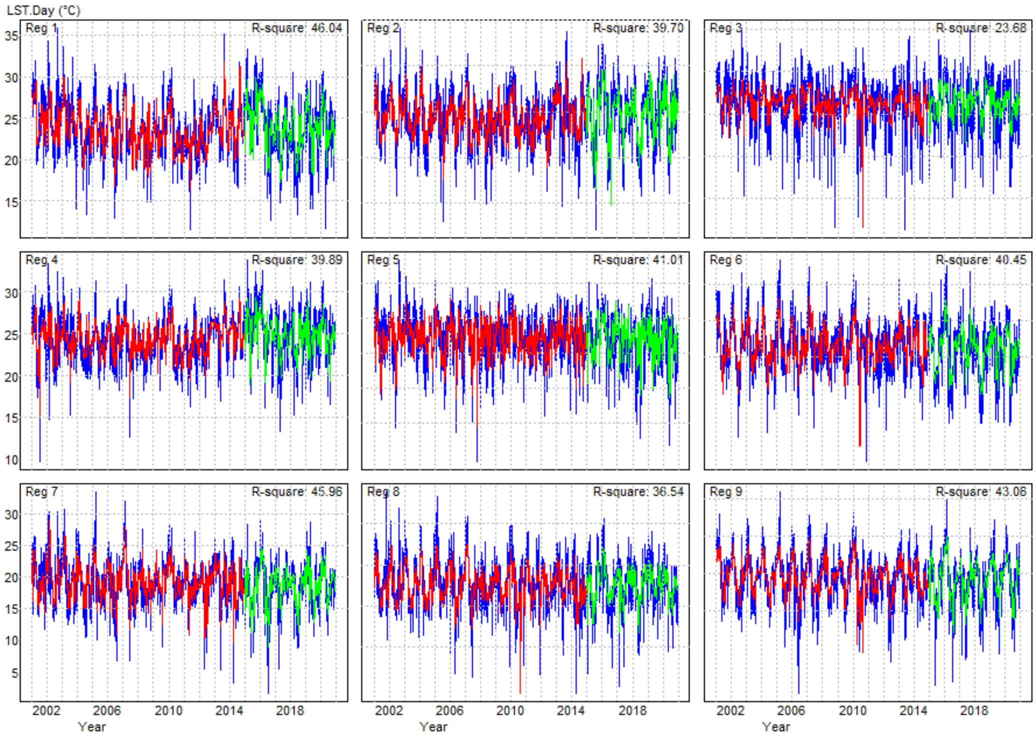

Figure 3.7 The plots of predicted against original values of LST using Multiple Linear Regression for 9 regions

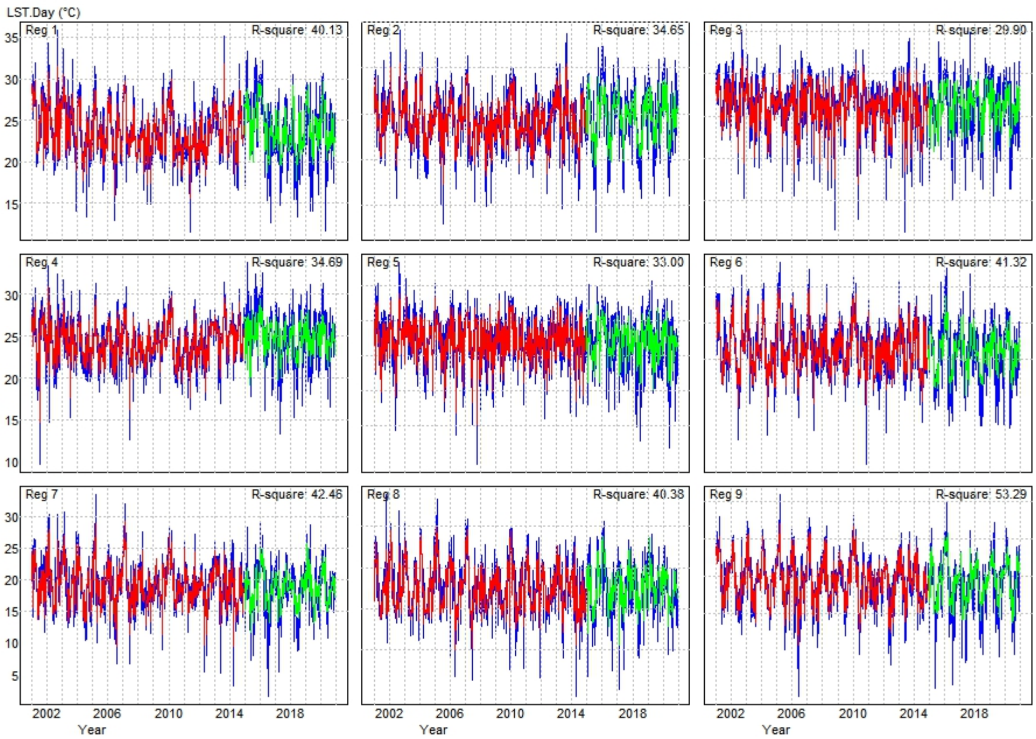

Figure 3.8 The plots of predicted against original values of LST using Random Forest for 9 regions

3.5 Models performance comparison

To evaluate the performance of the obtained models, the results of each model will be compared with training and testing datasets (original datasets) using R square and RMSE as Table 3.4.

Table 3.4 The RMSE and R-squared for each region

	Multiple Linear Regression			Random Forest		
Region	**R-square (%)**	**RMSE**		**R-square (%)**	**RMSE**	
		Training	**Testing**		**Training**	**Testing**
1	46.04	2.51	3.01	40.13	1.28	3.12
2	39.70	2.38	2.60	34.65	1.19	2.66
3	23.68	2.91	2.93	29.90	1.36	2.98
4	39.89	2.28	2.70	34.69	1.15	2.84
5	41.01	2.85	3.25	33.00	1.46	3.39
6	40.45	3.05	3.13	41.32	1.51	3.39
7	45.65	3.02	3.01	42.46	1.49	3.23
8	36.54	2.69	2.56	40.36	1.29	2.60
9	43.06	2.61	2.97	53.29	1.16	2.87

Table 3.4 shows the obtained R-square and RMSE values for all regions. It can be seen that the RF model gained the smallest RMSE from testing both training and testing data sets. The RMSE value of the MLR model was between 2.28 and 3.05 and between 2.56 and 3.35 for the training and testing data sets, respectively. Whereas those of the RF model were between 1.16 and 1.51 and between 2.60 and 3.39 for training and testing data sets, respectively. The R-square values of the MLR model were between 23.68 % and 45.65 %, while those of the RF model were between 29.90 % and 53.29 %.

Chapter 4

Conclusions and Discussions

The last chapter concludes the overall research results by applying statistical models and data visualization of land surface temperature in Bogota. The discussion of the findings, limits of the research, and future studies for technique improvement.

4.1 Discussion

This study used powerful statistical methods to investigate the seasonal patterns and trends of average 8-day LST in the upper north of Bogota, Colombia, from 2001 to 2020. The LST data fit well with the cubic spline function, and the appropriate number and location of knots provided a satisfactory fit to the LST data. This study found that all the LST had seasonal patterns similar for most regions, with the coldest period happening in the middle of the year and the hottest periods occurring in December and March. The lowest temperature occurs in the middle of the year.

The cubic spline function based on this research was fitted to depict the seasonal pattern and trend of the average 8-day LST in the upper north of Bogota from 2001 to 2020. A similar study by Fitrahanjani et al. (2021) employed the cubic spline on the LST data to observe the seasonal pattern and trend of the daylight data. Another consistency by Abdulmana et al. (2022) employed the cubic spline function to derive seasonality from the LST time series. The first and second derivatives of fitting splines are continuous, which gives them strong stability, smoothness, and high accuracy (Molinari et al., 2004).

A simple linear regression was employed to examine the trend of LST. This research found that the temperature increased in regions 2 and 4. Robledo-Buitrago et al. (2021) showed that this region is in the municipality of Facatativa, in the condition of Cundinamarca. The average temperature was between 9.2 °C and 14.0 °C, with an increasing trend of 0.00 °C/year to the west and 0.03 °C/year to the east.

The multiple linear regressions used to investigate relationships between LST and NDVI found positive correlations in all regions of Bogota. Sun and Kafatos (2007) discovered a positive correlation between LST and NDVI. According to Yue et al. (2007), the mean LST and NDVI values associated with different land-use categories varied substantially. Gorgani et al. (2013) concluded that the correlation between NDVI and LST is negative. This negative association between NDVI and LST is useful for studying the urban climate (Yuan and Bauer, 2007). According to Weng et al. (2004), there is a significantly higher negative association between the vegetation fraction and LST than previously reported. However, a recent study by Karnieli et al. (2006) found that the northern ecosystems at high latitudes have positive relationships between LST and NDVI.

The multiple linear regression and RF methods for sorting important LST variables showed the same results for all regions. NDVI is an important factor related to LST. Sorting variables after NDVI in regions 1, 3, and 4 are lag terms 2, 3, and 1, respectively. Regions 6, 7, 8, and 9 are lag terms 2, 1, and 3, respectively. Region 1 includes lag terms 3, 2, and 1, respectively. Furthermore, region 5 is lag term 1, 2, and 3, respectively. For the models' performance comparison, recent research by Xie et al. (2021) showed that the RF model did much better than the multiple linear regression model because it had much lower error indices (RMSE).

The results of each model were compared with the training and testing datasets (from which they were originally derived) using R-square and RMSE to assess the efficacy of the models that were created.

4.2 Conclusions

The objectives of this study were to analyze the trend of LST change and investigate the predictive models and factors related to LST variability in the upper north of Bogota, Columbia, by using RMSE and R-square as a measurement. The 8-day observation data were obtained from the NASA website.

This study concludes that the seasonal patterns of LST in the upper north of Bogota, Colombia had similar seasonal patterns with the highest levels during summer (December and March). The overall trend of LST has been decreasing over the last 20 years of the study. It was observed that the average temperature in the upper north of Bogota decreases slightly by 0.021 °C every year. The NDVI is one of the most important factors that provide a role in the change of LST. Based on the RMSE and R-square values, the random forest is the best and most accurate way to make predictions.

4.3 Limitations and further study

There are several limitations to this study. Firstly, climate variables provide a better understanding of how NDVI and LST patterns occur at various locations. However, these climate variables were not available to be explored in this study. Despite this significant limitation, this study would serve as our guide for carrying out the research in the future. In future, it is proposed that machine learning techniques be used to create the LST prediction model and compare its performance to another model.

References

Abdulmana, S., Lim, A., Wongsai, S., and Wongsai, N. 2022. Effect of land cover change and elevation on decadal trend of land surface temperature: a linear model with sum contrast analysis. Theoretical and Applied Climatology. 1-12.

Beniston, M. 2003. Climatic Change in Mountain Regions: A Review of Possible Impacts. In Climate Variability and Change in High Elevation Regions: Past, Present & Future, Diaz, H.F., Advances in Global Change Research, Springer, Dordrecht, pp. 5-31.

Breiman, L. 2001. Random forests. Machine learning. 45(1), 5-32.

Corredor, C., Corredor, J.A., Osorio, S., Duran, D., and Sarmiento-Suarez, R. 2016. Cardiovascular disease emergency admissions associated with maximum temperature in Bogota from 2009 to 2013. International Society for Environmental Epidemiology. Doi:10.1289/isee.2016.4098

Deng, Y., Wang, S., Bai, X., Tian, Y., Wu, L., Xiao, J., and Qian, Q. 2018. Relationship among land surface temperature and LUCC, NDVI in typical karst area. Scientific Reports. 8(1), 1-12.

Dobbs, C., Hernandez-Moreno, A., Reyes-Paecke, S., and Miranda, M.D. 2018. Exploring temporal dynamics of urban ecosystem services in Latin America: The case of Bogota (Colombia) and Santiago (Chile). Ecological Indicators. 85, 68-80.

Espinoza Villar, J. C., Ronchail, J., Guyot, J. L., Cochonneau, G., Naziano, F., Lavado, W., and Vauchel, P. 2009. Spatio-temporal rainfall variability in the Amazon basin countries (Brazil, Peru, Bolivia, Colombia, and Ecuador). International Journal of Climatology. 29(11), 1574-1594.

Ferrelli, F., Huamantinco, M.A., Delgado, D.A., and Piccolo, M.C. 2018. Spatial and temporal analysis of the LST-NDVI relationship for the study of land cover changes and their contribution to urban planning in Monte Hermoso. Argentina. Documents d'Analisi Geografica, 64(1), 25–47.

Fitrahanjani, C., Prasetya, T.A.E., and Indawati, R. 2021. A statistical method for analysing temperature increase from remote sensing data with application to Spitsbergen Island. Modeling Earth Systems and Environment. 7(1), 561-569.

Ghobadi, Y., Pradhan, B., Shafri, H.Z.M., and Kabiri, K. 2015. Assessment of spatial relationship between land surface temperature and landuse/cover retrieval from multi-temporal remote sensing data in South Karkheh Sub-basin, Iran. Arabian Journal of Geosciences. 8(1), 525-537.

Gidey, E., Dikinya, O., Sebego, R., Segosebe, E., and Zenebe, A. 2018. Using drought indices to model the statistical relationships between meteorological and agricultural drought in raya and its environs, Northern Ethiopia. Earth Systems and Environment. 2(2), 65-79.

Gorgani, S.A., Panahi, M., and Rezaie, F. 2013. The Relationship between NDVI and LST in the urban area of Mashhad, Iran. International Conference on Civil Engineering Architecture and Urban Sustainable Development, Tabriz, Iran, November , 27-28, 51.

Govil, H., Guha, S., Dey, A., and Gill, N. 2019. Seasonal evaluation of downscaled land surface temperature: A case study in a humid tropical city. Heliyon. 5(6), 1-15.

Goward, S.N., Xue, Y., and Czajkowski, K.P. 2002. Evaluating land surface moisture conditions from the remotely sensed temperature/vegetation index measurements: An exploration with the simplified simple biosphere model. Remote Sensing of Environment. 79(2-3), 225-242.

Guha, S., and Govil, H. 2021. An assessment on the relationship between land surface temperature and normalized difference vegetation index. Environment, Development and Sustainability. 23(2), 1944-1963.

Guha, S., Govil, H., and Diwan, P. 2020. Monitoring LST-NDVI relationship using Premonsoon Landsat datasets. Advances in Meteorology. 2020, 1-15.

Guha, S., Govil, H., Dey, A., and Gill, N. 2018. Analytical study of land surface temperature with NDVI and NDBI using Landsat 8 OLI and TIRS data in Florence and Naples city, Italy. European Journal of Remote Sensing. 51(1), 667-678.

Hao, B., Ma, M., Li, S., Li, Q., Hao, D., Huang, J., and Han, X. 2019. Land use change and climate variation in the three gorges reservoir catchment from 2000 to 2015 based on the Google Earth Engine. Sensors. 19(9), 1-24.

Hao, X., Li, W., & Deng, H. (2016). The oasis effect and summer temperature rise in arid regions-case study in Tarim Basin. Scientific Reports, 6(1). 1-9.

Hastie, T., Tibshirani, R., and Friedman, J. 2009. Random Forests. The Elements of Statistical Learning. Springer Series in Statistics. Springer, New York, NY, pp. 587-604.

Hou, G. L., Zhang, H.Y., Wang, Y.Q., Qiao, Z.H., and Zhang, Z.X. 2010. Retrieval and spatial distribution of land surface temperature in the middle part of Jilin province based on MODIS data. Scientia Geographica Sinica 30(3), 421-427.

Jansky, L., Ives, J.D., Furuyashiki, K., a Watanabe, T. 2002. Global mountain research for sustainable development. Global Environmental Change. 12(3), 231-239.

Julien, Y., Sobrino, J.A., and Verhoef, W. 2006. Changes in land surface temperatures and NDVI values over Europe between 1982 and 1999. Remote Sensing of Environment, 103(1). 43-55.

Karimi, N., Ng, K.T.W., and Richter, A. 2021. Prediction of fugitive landfill gas hotspots using a random forest algorithm and Sentinel-2 data. Sustainable Cities and Society. 73, 1-11.

Karnieli, A., Bayasgalan, M., Bayarjargal, Y., Agam, N., Khudulmur, S., and Tucker, C. J. 2006. Comments on the use of the vegetation health index over Mongolia. International Journal of Remote Sensing. 27(10), 17-24.

Kaufmann, R.K., Zhou, L., Myneni, R.B., Tucker, C.J., Slayback, D., Shabanov, N.V., and Pinzon, J. 2003. The effect of vegetation on surface temperature: A statistical analysis of NDVI and climate data. Geophysical Research Letters. 30(22), 1-4.

Kavitha, S., Varuna, S., and Ramya, R. 2016. A comparative analysis on linear regression and support vector regression. International Conference on Green Engineering and Technologies. Coimbatore, November 19, 2016, 1-5.

Leroy, D. 2019. Farmers' Perceptions of and Adaptations to Water Scarcity in Colombian and Venezuelan Páramos in the Context of Climate Change. Mountain Research and Development. 39(2), 21-34.

Li, L., Rong, M., and Zhang, G. 2015. An Internet of Things QoE evaluation method based on multiple linear regression analysis. International Conference on Computer Science and Education. Cambridge, UK, July 22-24, 2015, 25-28.

Li, W.F., Cao, Q.W., Kun, L., and Wu, J.S. 2017. Linking potential heat source and sink to urban heat island: Heterogeneous effects of landscape pattern on land surface temperature. Science of the Total Environment. 586, 457–465.

Liang, S., Wang, D., He, T., and Yu, Y. 2019. Remote sensing of earth's Earth's energy budget: Synthesis and review. International Journal of Digital Earth. 12(7), 737-780.

Madanian, M., Soffianian, A.R., Koupai, S.S., Pourmanafi, S., and Momeni, M. 2018. The study of thermal pattern changes using Landsat-derived land surface temperature in the central part of Isfahan province. Sustainable Cities and Society. 39, 650-661.

Martinez-Bello, D., López-Quilez, A., and Prieto, A.T. 2018. Spatiotemporal modeling of relative risk of dengue disease in Colombia. Stochastic Environmental Research and Risk Assessment. 32(6), 1587-1601.

McGranahan, G., Balk, D., and Anderson, B. 2007. The rising tide: assessing the risks of climate change and human settlements in low elevation coastal zones. Environment and Urbanization. 19(1), 17-37.

Molinari, N., Durand, J.F., and Sabatier, R. 2004. Bounded optimal knots for regression splines. Computational Statistics & Data Analysis. 45(2), 159-178.

Musse, M.A., Barona, D.A., and Rodriguez, L.M.S. 2018. Urban environmental quality assessment using remote sensing and census data. International Journal of Applied Earth Observation and Geoinformation. 71, 95-108.

Natarajan, S., Rodriguez, J., and Vellei, M. 2015. A field study of indoor thermal comfort in the subtropical highland climate of Bogota, Colombia. Journal of Building Engineering. 4, 237-246.

Ogashawara, I., Li, L., and Moreno-Madriñán, M.J. 2019. Spatial-temporal assessment of environmental factors related to dengue outbreaks in Sao Paulo, Brazil. GeoHealth. 3(8), 202-217.

Parra-Henao, G., Quiros-Gomez, O., Jaramillo-O, N., and Cardona, A. S. 2016. Environmental determinants of the distribution of Chagas disease vector

Triatoma dimidiata in Colombia. The American Journal of Tropical Medicine and Hygiene. 94(4), 767-774.

Qu, C., Ma, J.H., Xia, Y.Q., and Fei, T. 2014. Spatial distribution of land surface temperature retrieved from MODIS data in Shiyang river Basin. Arid Land Geography. 37, 125–133.

R Core Team 2020. A language and environment for statistical computing, R Foundation for Statistical Computing, Vienna, Austria.

Rahman, M.T.U., and Esha, E.J. 2022. Prediction of land cover change based on CA-ANN model to assess its local impacts on Bagerhat, southwestern coastal Bangladesh. Geocarto International. 37(9), 2604-2626.

Ramirez-Aguilar, E.A., and Souza, L.C.L. 2019. Urban form and population density: influences on urban heat island intensities in Bogotá, Colombia. Urban Climate. 29, 1-19.

Raynolds, M.K., Comiso, J.C., Walker, D.A., and Verbyla, D. 2008. Relationship between satellite-derived land surface temperatures, arctic vegetation types, and NDVI. Remote Sensing of Environment. 112(4), 1884-1894.

Robledo-Buitrago, D.A., Polanco-Puerta, M.F., De Luque-Villa, M., Mesa-Caro, M., and Calderón-Ricardo, C.A. 2021. Climate Change Trends in Colombia: A Case Study in Facatativá, Cundinamarca. International Journal of Sustainable Development and Planning. 16(3), 535-542.

Romero, C., Paniagua-Zambrana, N.Y., and Bussmann, R. W. 2020. Ethnobotany of Mountain Regions–Andes–Colombia and Ecuador. In Ethnobotany of the Andes, Zambrana, N., Bussmann, R., Ethnobotany of Mountain Regions. Springer, Cham, pp. 83-104.

Seto, K.C., Fleishman, E., Fay, J.P., and Betrus, C.J. 2004. Linking spatial patterns of bird and butterfly species richness with Landsat TM derived NDVI. International Journal of Remote Sensing. 25(20), 4309-4324.

Sharma, I., Ueranantasun, A., and Tongkumchum, P. 2018. Modeling of satellite data to identify the seasonal patterns and trends of vegetation index in Kathmandu Valley, Nepal from 2000 to 2015. Jurnal Teknologi. 80(4), 1-9.

Shivers, S.W., Roberts, D.A., and McFadden, J.P. 2019. Using paired thermal and hyperspectral aerial imagery to quantify land surface temperature variability and assess crop stress within California orchards. Remote Sensing of Environment. 222, 215-231.

Siddique, N.P., and Ghaffar, A. 2019. Spatial and Temporal relationship between NDVI and Land Surface Temperature of Faisalabad city from 2000-2015. European Online Journal of Natural and Social Sciences. 8(1), 55-64.

Son, N.T., Chen, C.F., Chen, C.R., Chang, L.Y., and Minh, V.Q. 2012. Monitoring agricultural drought in the Lower Mekong Basin using MODIS NDVI and land surface temperature data. International Journal of Applied Earth Observation and Geoinformation. 18, 417-427.

Speiser, J. L., Miller, M.E., Tooze, J., and Ip, E. 2019. A comparison of random forest variable selection methods for classification prediction modeling. Expert Systems with applications. 134, 93-101.

Sruthi, S., and Aslam, M.M. 2015. Agricultural drought analysis using the NDVI and land surface temperature data; a case study of Raichur district. Aquatic Procedia. 4, 1258-1264.

Sun, D., and Kafatos, M. 2007. Note on the NDVI-LST relationship and the use of temperature-related drought indices over North America. Geophysical Research Letters. 34(24), 1-4.

Testa, S., Mondino, E.C.B., and Pedroli, C. 2014. Correcting MODIS 16-day composite NDVI time-series with actual acquisition dates. European Journal of Remote Sensing. 47(1), 285-305.

Voogt, J.A., and Oke, T.R. 2003. Thermal remote sensing of urban climates. Remote Sensing of Environment. 86(3), 70-84.

Wan, Z., Wang, P., and Li, X. 2004. Using MODIS land surface temperature and normalized difference vegetation index products for monitoring drought in the southern Great Plains, USA. International Journal of Remote Sensing. 25(1), 61-72.

Wang, C., Yang, J., Myint, S.W., Wang, Z.H., and Tong, B. 2016. Empirical modeling and spatio-temporal patterns of urban evapotranspiration for the Phoenix metropolitan area, Arizona. GIScience & Remote Sensing. 53(6), 778-792.

Wang, R., Gao, W., and Peng, W. 2020. Downscale MODIS land surface temperature based on three different models to analyze surface urban heat island: a case study of Hangzhou. Remote Sensing. 12(13), 1-22.

Weng, Q., Lu, D., and Schubring, J. 2004. Estimation of land surface temperature–vegetation abundance relationship for urban heat island studies. Remote Sensing of Environment. 89(4), 467-483.

Wilson, N. R., & Norman, L. M. (2018). Analysis of vegetation recovery surrounding a restored wetland using the normalized difference infrared index (NDII) and normalized difference vegetation index (NDVI). International Journal of Remote Sensing. 39(10), 3243-3274.

Wongsai, N., Wongsai, S. and Huete, A.R. 2017. Annual seasonality extraction using the cubic spline function and decadal trend in temporal daytime MODIS LST data. Remote Sensing. 9(12). Doi: 10.3390/rs9121254

Xie, X., Wu, T., Zhu, M., Jiang, G., Xu, Y., Wang, X., and Pu, L. 2021. Comparison of random forest and multiple linear regression models for estimation of soil extracellular enzyme activities in agricultural reclaimed coastal saline land. Ecological Indicators. 120, 1-9. Doi:10.1016/j.ecolind.2020.106925

Xu, Y., Knudby, A., and Ho, H.C. 2014. Estimating daily maximum air temperature from MODIS in British Columbia, Canada. International Journal of Remote Sensing. 35(24), 8108-8121.

Yuan, F., and Bauer, M. E. 2007. Comparison of impervious surface area and normalized difference vegetation index as indicators of surface urban heat island effects in Landsat imagery. Remote Sensing of Environment. 106(3), 75-86.

Yuan, X. L. 2017. Vegetation changes and land surface feedbacks drive shifts in local temperatures over Central Asia. Scientific Report. 7, 3287.

Yue, W., Xu, J., Tan, W., and Xu, L. 2007. The relationship between land surface temperature and NDVI with remote sensing: application to Shanghai Landsat 7 ETM+ data. International Journal of Remote Sensing. 28(15), 3205-3226.

Zhang, G., Yao, T., Xie, H., Qin, J., Ye, Q., Dai, Y., and Guo, R. 2014. Estimating surface temperature changes of lakes in the Tibetan Plateau using MODIS LST data. Journal of Geophysical Research: Atmospheres. 119(14), 52-67.

Zhang, J., and Wang, Y. 2008. Study of the relationships between the spatial extent of surface urban heat islands and urban characteristic factors based on Landsat ETM+ data. Sensors. 8(11), 7453-7468.

Zhou, Y., Shi, T.M., Hu, Y.M., and Liu, M. 2011. Relationships between land surface temperature and normalized difference vegetation index based on urban land use type. Chinese Journal of Ecology. 30, 1504–1512.

Zwally, H.J., Schutz, B., Abdalati, W., Abshire, J., Bentley, C., Brenner, A., and Thomas, R. 2002. ICESat's laser measurements of polar ice, atmosphere, ocean, and land. Journal of Geodynamics. 34(3-4), 405-445.

Appendix

Thai Journal of Mathematics
Special Issue: The 17th IMT-GT ICMSA 2021
Pages 106–116 (2022)
http://thaijmath.in.cmu.ac.th

ISSN 1686-0209

Land Surface Temperature Prediction in Chiang Mai Province Thailand Using MODIS LST Data

Khodeeyoh Kasoh[1], Salang Musikasuwan[1,*] and Rattikan Saelim[1]

[1] *Department of Mathematics and Computer Science, Faculty of Science and Technology, Prince of Songkla University, Pattani Campus, Pattani, Thailand 94000*
e-mail : 6220320002@psu.ac.th (K. Kasoh); salang.m@psu.ac.th (S. Musikasuwan); rattikan.s@psu.ac.th (R. Saelim)

Abstract The temperature increase is one of the indicators of global warming. Therefore, Land Surface Temperature (LST) trends can be used to identify climate change. The objectives of this study were (i) to analyze the trend of LST change in Chiang Mai province (ii) to investigate the suitable models for predicting LST in Chiang Mai, Thailand. The observation data used in this study were obtained from Moderate Resolution Imaging Spectroradiometer (MODIS) LST Data on the National Aeronautics and Space Administration (NASA) website and referred to as LST MODIS. The data were collected every 8 days from January 1, 2001, to December 27, 2020 (920 observations).The data were split into 70%-30% proportions for training and checking datasets, respectively. In this study, the simple linear regression was used to analyze trends of the average LST change over 20 years. It is found that, the average LST in Chiang Mai province has been slightly increasing around 0.0184 degrees Celsius per year. The autoregressive integrated moving average (ARIMA) model has been applied for predicting LST, and the Root Mean Squared Error (RMSE) and coefficient of determination (R-squared) were used to measure the model performance. The results showed that ARIMA(2,0,0) model had the smallest RMSE for both training and checking data sets. In addition, all fitted ARIMA models can describe the LST with R-squared ranging from 0.6404 - 0.7871.

MSC: 49K35; 47H10; 20M12

Keywords: land surface temperature; climate change; autoregressive integrated moving average

Submission date: 31.01.2022 / Acceptance date: 31.03.2022

1. Introduction

The changes in Land Surface Temperature (LST) on sub-continental or regional sizes reveal distinct characteristics. In addition, the regional climate is more complex than the global climate since it is impacted by ocean-atmospheric circulation, land cover, and feedback processes. Thus, the regional climate is important for the environment and economic output [1].

*Corresponding author.

Published by The Mathematical Association of Thailand.

Time series analysis is used to develop mathematical models for the purpose of computing statistics from data on climatic variables using the autoregressive integrated moving average (ARIMA) model. Since the 1970s, time series analysis has rapidly advanced in theory and practice for the purpose of predicting and controlling various climatic factors such as precipitation, temperature, and others [2]. In 2014, Wang et al. [3] proposed the predictive model for monthly precipitation at the Lanzhou station in Lanzhou, China, using the enhanced ARIMA model. The findings indicated that the revised model is much more accurate than the seasonal model, with a mean residual of 9.41 mm and a forecast accuracy of 21%. Later in 2015, Bari et al. [4] forecasted monthly precipitation for Sylhet, Bangladesh, using the ARIMA model. They discovered that the ARIMA(0,0,1)(1,1,1) technique was the most efficient for forecasting future precipitation with a 95% confidence interval. El-Mallah et al. [5] used the Box-Jenkins method to predict the annual warming trend in 2016 and found that ARIMA(3,1,2) and ARIMA(3,2,3) were capable of predicting non-seasonal linear and quadratic trend models with results that followed their predicted patterns with correlation values of around 80% for both models. Morever, in 2017 Wongsai et al. [6] presented the analysis of annual seasonality extraction using the cubic spline function and decadal trend in temporal daytime Moderate Resolution Imaging Spectroradiometer (MODIS) LST data. Later in 2018, Sharma et al. [7] analyzed LST data from 2000 to 2015 to determine seasonal variations in the Kathmandu Valley of Nepal. They discovered that the patterns were significantly associated with altitude (p-value $< .01$). In the same year, Ruchiraset and Tantrakarnapa [8] conducted the study about time-series modeling of pneumonia admissions and its association with air pollution and climate variables in Chiang Mai Province, Thailand. As Chiang Mai Province faced with the variation of climate change, the study of trend and predicting model for temperature would be considered to conduct and analyze.

Chiang Mai locates in the northern Thailand. It is one of Thailand's major cities with 696 kilometers north of Bangkok. Its landscape is a mountain-rimmed basin [9]. Chiang Mai is one of cities that faced with extremely air pollution. There were some studies focused on this city. In 2012, Gou et al. [10] reported that particulate matter and ozone are the principal ambient contaminants in Chiang Mai. Suwanprasit [11] had analyzed the changes in land use and LST across Mueang Chiang Mai District, Thailand using satellite photos from Landsat TM and ETM+. The findings demonstrated that during the research period, the city's land usage changed dramatically, the maximum LST values found at bare ground area, and lowest LST values found at the forest, farm, and water resource classes. The temperature difference between cities and suburbs was 1 - 2C in 1994 and 5-8C in 2014.

Chiang Mai is the top destination for domestic and foreign tourists, and the surface temperature is one of the important factors that tourists use for making their decisions to visit Chiang Mai. The short-term predictive model would be suggested for both tourists and tourism agencies. Hence, this study has been conducted to analyze the trend of LST change in Chiang Mai Province using MODIS LST from the NASA website and investigated the suitable models for predicting short-term LST in Chiang Mai Province. The rest of this paper is organized as follows: Section 2 explains the data and methods used in this study. The results of this study have been presented in Section 3. Finally, Section 4 describes our discussion and conclusion.

2. MATERIALS AND METHODS

2.1. CONCEPTUAL FRAMEWORK

The first step in our investigation was to get LST data from the NASA website. Because the original LST's unit was Kelvin and there were missing values, it was necessary to undertake data management. After that, the LST season was explored by averaging LST on the same day of the year. Following that, a simple linear regression was used to determine the trend of LST change in Chiang Mai. The ARIMA was used as a predictive model to fit the original LST. Finally, the model's performance was assessed by using the root mean square error (RMSE) and the coefficient of determination (R-squared).

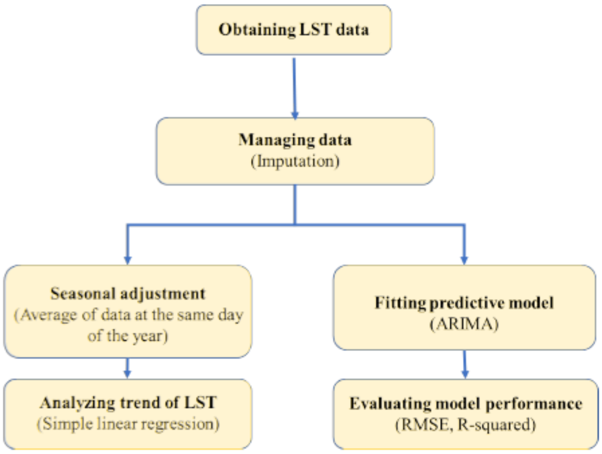

FIGURE 1. Conceptual Framework

2.2. STUDY AREA

Chiang Mai is the biggest city in northern Thailand. It is located at latitude 18.793867 and longitude 98.997116 and covering the area of 20,170 square kilometers. It is divided into 25 districts. There are 1,682,164 people living in the city, with 742,489 households. Chiang Mai has three seasons: winter (November to February), summer (March to May), and the rainy season (June to October) [8]. In this study, 9 regions in Chiang Mai province were selected (black dot in Figure 2). Each region comprising 49 pixels in 77 arrays as shown in the right panel of Figure 2.

2.3. DATA COLLECTION AND EXPLORATION

The LST data were obtained from MODIS on the NASA website using MOD11A2 product, which was collected every 8 days during January 1, 2001, and December 27, 2020 (in total, 920 data observations). LST data of 9 regions have been considered for this study. The LST units were converted to degrees Celsius by subtracting 273.15 from the Kelvin values. Figure 2 showed the time-series plots of LST for each region over 20 years. The time series plot of the 9 regions and the overall average (of all 9 regions) have been presented in Figure 3.

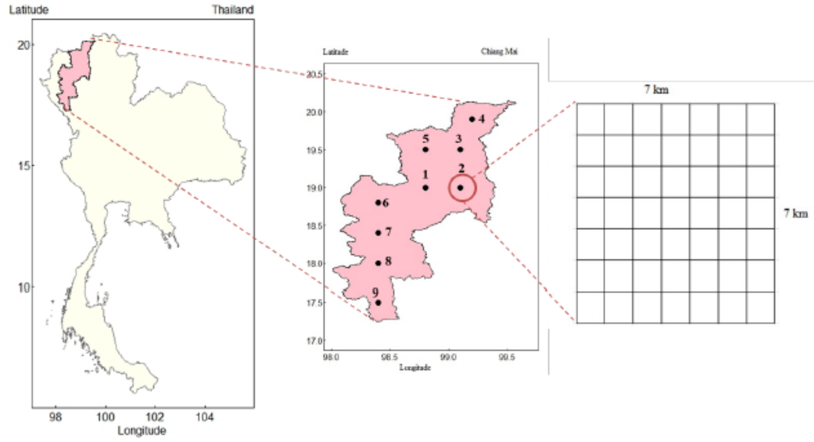

FIGURE 2. Study area for LST in urban area of Chiang Mai Province

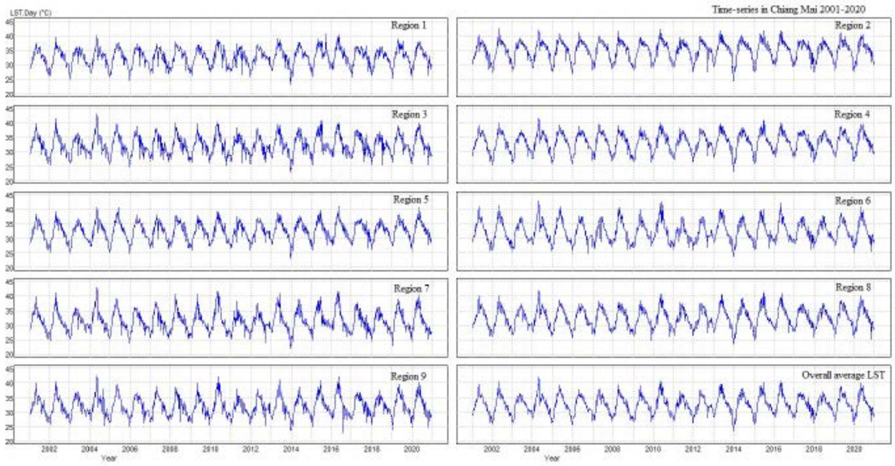

FIGURE 3. Time-series plots of LST for 9 regions and overall average LST

There are some missing values in the downloaded data. In this study, mean substitution has been selected for dealing with missing values. To construct the predicting models, the data have been divided into 70%-30% proportions for training and checking data sets for the 9 regions and the overall average LST. Training dataset has been used for constructing the predictive models, while checking dataset has been used for evaluating and validating the predictive models by considering the RMSE and R-squared.

2.4. METHODS

Simple linear regression was fitted to investigate the temperature trends. The simple linear regression model takes the following form (2.1):

$$\hat{y}_t = \beta_0 + \beta_1 t + \epsilon, \tag{2.1}$$

where $\hat{y}_t$ is the fitted LST, β_0 is the intercept, β_1 is the regression coefficient, t is the time (t=1,2,3,...,920) and ϵ is the error term.

Time series models have been built using stationary variables that have the same mean and variance across time. In principle, ARIMA models are the best models for forecasting a time-series. However, fitting a suitable model, estimating the parameters, and validating the model are all part of the process [12]. The best prediction model for all 9 regions and their average turned out to be ARIMA(2,0,0) whose general equation is: as shown in Equation 2.2.

$$\hat{y}_t = \mu + \phi_1 y_{t-1} + \phi_2 y_{t-2} + \epsilon_t, \tag{2.2}$$

where $\hat{y}_t$ is the predicted LST value at observation t, ϕ_1,ϕ_2 are coefficients of the lag variables, y_{t-1} and y_{t-2}, respectively. ϵ_t is the value not explained by the model.

After obtaining the appropriate models, the predicted value is calculated from the training and checking datasets and evaluating those models using RMSE as shown in Equation 2.3.

$$RSME = \sqrt{\sum_{t=1}^{n} \frac{(y_t - \hat{y}_t)^2}{n}}, \tag{2.3}$$

where n is the defined as the number of predicted data, t is the defined time, y_t is the observation at time t, and $\hat{y}_t$ is the predicted value. Finally, the final models were tested using R-squared to determine whether they fit well enough for the training dataset. Equation 2.4 shows the formula for calculating the R-squared value.

$$R^2 = 1 - \sum_{t=1}^{n} \frac{(\hat{y}_t - y_t)^2}{(y_t - \overline{y}_t)^2}, \tag{2.4}$$

where $\hat{y}_t$ is the predicted LST value at observation t, y_t is LST value, $\overline{y}_t$ is the mean of LST value.

3. RESULTS

3.1. SEASONAL PATTERNS ANALYSIS

To eliminate the effect of the seasonality, the seasonal adjustment has been performed. The stationary of LST can be checked at this process. The time series plot of original data (blue lines) and seasonal patterns (red curve) in Chiang Mai over 20 years were shown in Figure 4. While Figure 5 presented the time series plot of seasonal adjusted LST. After perfoming seasonal adjustment, all data were satisfied for applying with ARIMA model. LST increased slightly in all regions, including the overall average LST, after fitting the basic linear regression for each location.

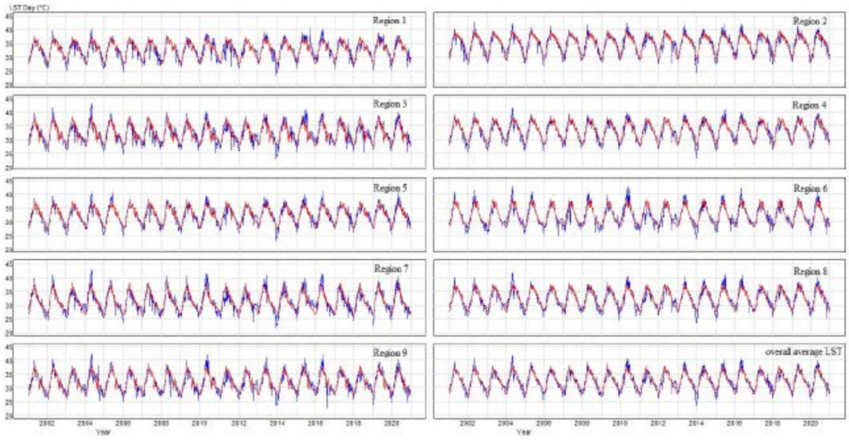

FIGURE 4. Time-series plots and seasonal patterns

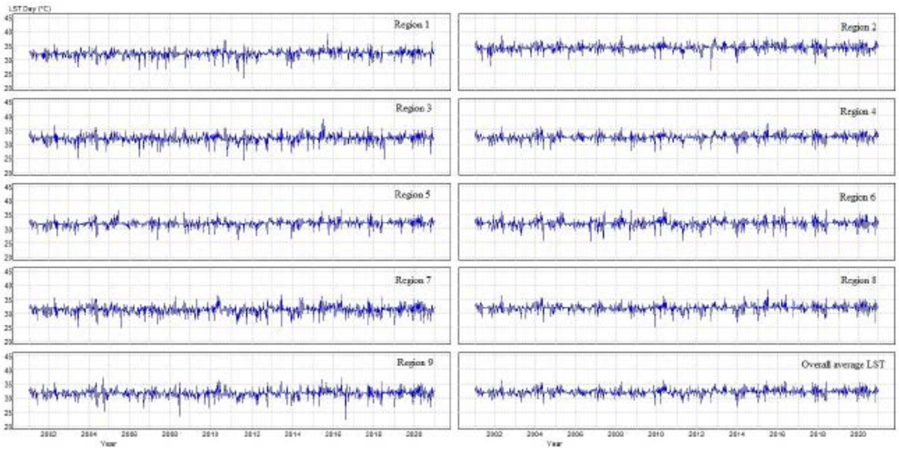

FIGURE 5. Time-series plots of LST after applied seasonal adjusted.

3.2. LAND SURFACE TEMPERATURE TREND ANALYSIS

After fitting the simple linear regression for each location, it was discovered that LST increased slightly in all regions, including the overall average LST. Each blue points represents original LST and red linear line represents the trend of LST for each region as showed in Figure 6.

3.3. LAND SURFACE TEMPERATURE PREDICTING MODELS

To construct the predictive models, the seasonally adjusted of training datasets will be used to create the ARIMA model by considering the graph of Autocorrelation Function (ACF) and Partial Autocorrelation Function (PACF) to determine the q and p parameters of ARIMA model as shown in Figure 7.

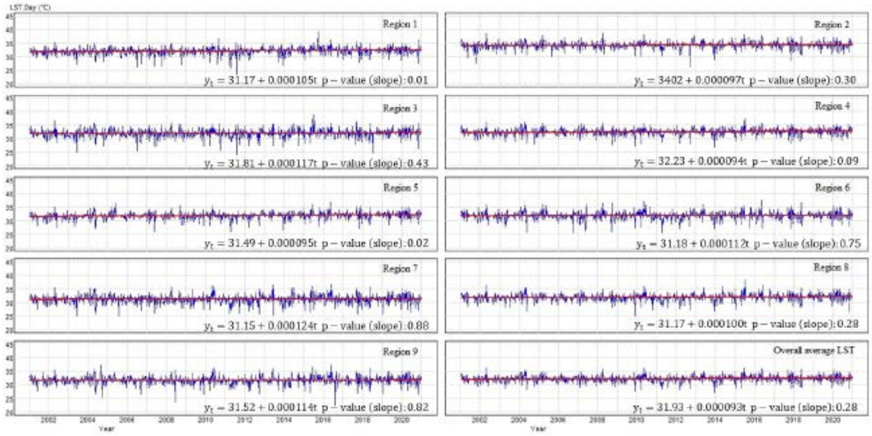

FIGURE 6. The red line showed the trend of LST change in Chiang Mai for 9 regions and overall average LST.

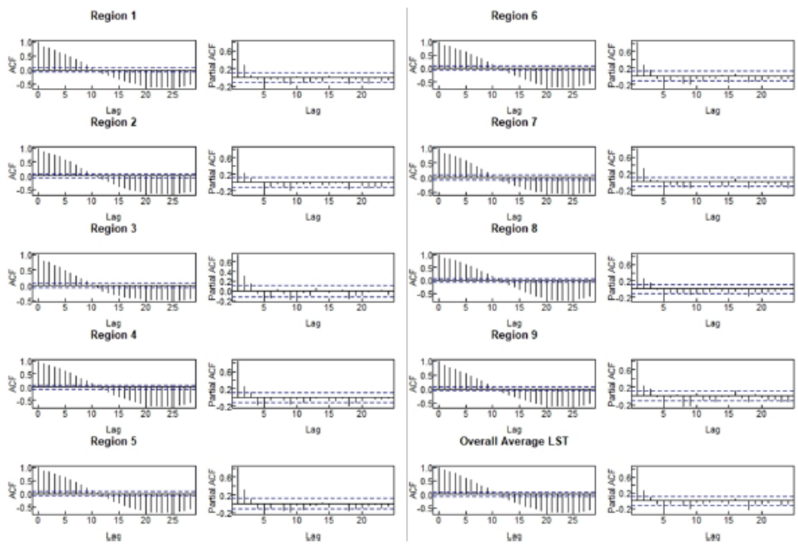

FIGURE 7. The graph of ACF and PACF for 9 regions and overall average LST

It was found that ARIMA(2,0,0) was the most suitable for dataset in all regions. The equations of ARIMA(2,0,0) for 9 region and overall average LST was given in Table 1. To evaluate the performance of the obtained models, the results of each model will be compared with testing and checking datasets (original datasets) using RMSE. Table 2 showed the obtained RMSE values for all regions and overall average LST. In fact, the obtained RMSE for training dataset for all regions varied between 1.40 and 1.96 degree Celsius, and for checking dataset varied between 1.51 and 2.07 degree Celsius. In addition, all fitted ARIMA models can describe the LST with R-squared ranging from 0.6404 to 0.7871.

TABLE 1. The equation of ARIMA (2,0,0) for each region and overall average LST

Region	Equation of ARIMA(2,0,0)
1	$\hat{y}_t$=3.8537+0.5501y_{t-1}+0.3304y_{t-2}
2	$\hat{y}_t$=3.2307+0.6108y_{t-1}+0.2959y_{t-2}
3	$\hat{y}_t$=4.5602+0.4996y_{t-1}+0.3576y_{t-2}
4	$\hat{y}_t$=2.6698+0.6491y_{t-1}+0.2697y_{t-2}
5	$\hat{y}_t$=2.9785+0.5693y_{t-1}+0.3380y_{t-2}
6	$\hat{y}_t$=3.0152+0.6433y_{t-1}+0.2630y_{t-2}
7	$\hat{y}_t$=3.2677+0.5176y_{t-1}+0.3778y_{t-2}
8	$\hat{y}_t$=2.8779+0.6327y_{t-1}+0.2783y_{t-2}
9	$\hat{y}_t$=4.1001+0.6561y_{t-1}+0.2148y_{t-2}
overall average LST	$\hat{y}_t$=2.6691+0.6440y_{t-1}+0.2735y_{t-2}

TABLE 2. TABLE 2 The RMSE for 9 region and overall average LST

Region	RMSE		R-squared
	Training	Checking	
1	1.64776	1.72194	0.7023
2	1.57787	1.65628	0.7558
3	1.95550	2.07311	0.6404
4	1.46398	1.51291	0.7904
5	1.52230	1.58928	0.7533
6	1.63139	1.66319	0.7662
7	1.80424	1.92773	0.7293
8	1.52475	1.65968	0.7726
9	1.77237	1.95997	0.6989
Overall Average LST	1.40722	1.53105	0.7871

The plots of predicted LST against original data for all regions using the ARIMA(2,0,0) model have been presented in Figure 8. Each blue line represents original LST, the red line represents predicted LST for training dataset and the green line represent predicted LST for checking dataset.

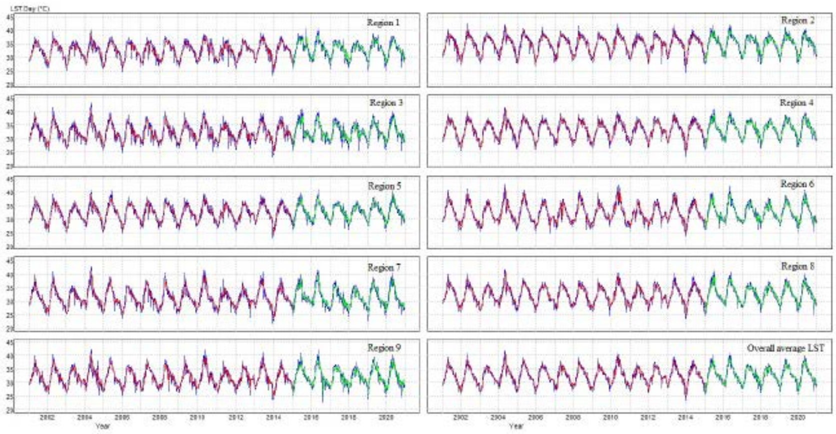

FIGURE 8. The plots of predicted against original values of LST using ARIMA(2,0,0) for region 1-9 and overall average LST

4. DISCUSSION AND CONCLUSION

The objectives of this study were to analyze the trend of LST change in Chiang Mai Province and investigate the suitable models for predicting land surface temperature in Chiang Mai, Thailand, by using RMSE as a measurement. The 8-day observation data were obtained from the NASA website.

By analyzing the data used in this study, the LST in Chiang Mai showed the maximum of 41.893 degrees Celsius, the minimum of 23.35 degrees Celsius, and the average of 32.61 degrees Celsius.

The simple linear regression had been used to analyze trend of the average LST change over 20 years. From the analysis, it was found that the LST of all regions approximately increase over 20 years. As an overall LST in Chiang Mai Province, the average LST has been slightly increasing around 0.0184 degrees Celsius each year. It should be noticed that region 2 has a greater LST than the other regions. This could be due to the fact that it covers the Chiang Mai city area, which is densely populated with high-rise buildings and has a high level of commuting. As a result, this research will provide evidence to policymakers so that they are aware of the impact of climate change in Chiang Mai.

In this study, the LST observations had been divided into 2 partitions as 70%:30% for training and checking datasets, respectively. To investigate the suitable predictive models for the LST, the ARIMA model has been applied with training dataset. The RMSE and R-squared were used to measure the performance of the models. The results showed that ARIMA(2,0,0) model had the smallest RMSE while testing with both training and checking datasets. It can be suggested that our final ARIMA(2,0,0) model was suitable for predicting LST in Chiang Mai Province. Furthermore, the model derived from the average of overall LST can be used to represent the entire province of Chiang Mai. Noted that, this study assessed only LST data in Chiang Mai Province, so the finding of this study did not provide a general conclusion for other locations. For future work, it would be suggested that machine learning techniques can be applied for developing the LST predictive model to compare the performance with ARIMA.

Acknowledgements

This work was partially supported by Faculty of Science and Technology, and Graduate School, Prince of Songkla University, Pattani Campus, Thailand. We would also like to express our gratitude to the referees for their helpful suggestions, which significantly improved the manuscript.

References

[1] G. Yan, D. Wen-Jie, R. Fu-Min, Z. Zong-Ci, H. Jian-Bin, Surface air temperature over China with CMIP5 and CMIP3, Advances in Climate Change Research 4 (3) (2013) 145-152.

[2] K.H. Machekposhti, H. Sedghi, A. Telvari, H. Babazadeh, Modeling climate variables of rivers basin using time series analysis (case study: Karkheh river basin at Iran), Civil Engineering Journal 4 (1) (2018) 78-92.

[3] H.R. Wang, C., X. Lin, J. Kang, An improved ARIMA model for precipitation simulations, Nonlinear Processes in Geophysics 21 (6) (2014) 1159-1168.

[4] S.H. Bari, M.T. Rahman, M.M. Hussain, S. Ray, Forecasting monthly precipitation in Sylhet city using ARIMA model, Civil and Environmental Research 7 (1) (2015) 69-77.

[5] E.S. El-Mallah, S.G. Elsharkawy, Time-series modeling and short term prediction of annual temperature trend on Coast Libya using the Box-Jenkins ARIMA Model, Advances in Research 6 (5) (2016) 1-11.

[6] N. Wongsai, S. Wongsai, A.R. Huete, Annual seasonality extraction using the cubic spline function and decadal trend in temporal daytime MODIS LST data, Remote Sensing 9 (12) (2017) 1-17.

[7] I. Sharma, A. Ueranantasun, P. Tongkumchum, Modeling of land surface temperatures to determine temperature patterns and detect their association with altitude in the Kathmandu Valley of Nepal, Chiang Mai University Journal of Natural Sciences 17 (4) (2018) 275-288.

[8] A. Ruchiraset, K. Tantrakarnapa, Time series modeling of pneumonia admissions and its association with air pollution and climate variables in Chiang Mai province, Thailand, Environmental Science and Pollution Research 25 (33) (2018) 33277-33285.

[9] N. Kammuang-Lue, P. Sakulchangsatjatai, P. Sangnum, P. Terdtoon, Influences of population, building, and traffic densities on urban heat island intensity in Chiang Mai City, Thailand, Thermal Science 19 (2) (2015) 445-455.

[10] Y. Guo, K. Punnasiri, S. Tong, Effects of temperature on mortality in Chiang Mai city, Thailand: a time series study, Environmental Health 11 (1) (2012) 1-9.

[11] C. Suwanprasit, Pattern of land-use change and urban heat island during 20 years in Chiang Mai, Thailand, International Multidisciplinary Scientific GeoConference Surveying Geology and Mining Ecology Management 41 (17) (2017) 535-542.

[12] R. Anokye, E. Acheampong, I. Owusu, E. Isaac Obeng, Time series analysis of malaria in Kumasi: using ARIMA models to forecast future incidence, Cogent Social Science 4 (1) (2018) 1-13.

VITAE

Name Miss. Khodeeyoh Kasoh

Student ID 6220320002

Educational Attainment

Degree	Name of Institution	Year of Graduation
B. (Applied Mathematics)	Prince of Songkla University	2019

List of Publication and Proceeding

Publication

Kasoh, K., Musikasuwan, S., and Saelim, R. 2022. Land Surface Temperature Prediction in Chiang Mai Province Thailand Using MODIS LST Data. Thai Journal of Mathematics**,** 2022, 106-116.

Proceeding

Kasoh, K., Musikasuwan, S., and Saelim, R. Land Surface Temperature Prediction in Chiang Mai Province Thailand Using MODIS LST Data. Proceeding of International Conference on Mathematics, Statistics and Their Applications Conference, Pattani, Thailand, December 12-14, 2021